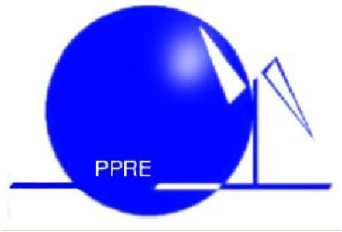

Generation of a CALIPSO climatology of near-surface boundary layer aerosols for solar energy applications

by

Diana Rocío Mancera Guevara

Date and Place of Birth:

29^{th} September 1980 in Bogotá / Colombia

Master Thesis

in the Postgraduate Programme

RENEWABLE ENERGY

In cooperation with

German Aerospace Center DLR

German Remote Sensing Data Center - Oberpffafenhoffen

Energy and Semiconductor Research Laboratory

Department of Physics

Faculty of Mathematics & Science

Carl von Ossietzky University

Oldenburg / Germany

Day of Examination:	26^{th} March 2013
1. Examiner:	Prof. Dr. Jürgen Parisi
2. Examiner:	Dr. Detlev Heinemann

To God Father, Son and Holy Spirit, source of life, love and light on my path.

To the blessed Virgin Mary, for her sweet protection and guidance.

To my family, my inspiration, strength and joy. My parents, Jorge and Alba, total loving dedication, who give everything for their daughters and have been working for our dreams to come true even before we were aware of them . My sister and friend Patricia, tireless support and confidence for me. To my grandparents Jesús, María y Gabriel, encouragement and light from the heaven and to my grandmother María, a model of fortitude. Thank you all for your unconditional love.

A mi familia, mi inspiración, fortaleza y alegría. Mis papás, Jorge y Alba, amorosa y total entrega, quienes dan todo por sus hijas y han trabajado para que nuestros sueños se hagan realidad aun desde antes de que fueramos conscientes de ellos. A mi hermana y amiga Patricia, incansable apoyo y confianza para mí. A mis abuelitos Jesús, María y Gabriel, ánimo y luz desde el cielo y a mi abuelita María ejemplo de fortaleza. Gracias a todos por su amor incondicional.

To Mauricio, fellow in my adventure... Thank you for your company, patience and love, and for your creative support.

To Colombia, my country, one of the most powerful engines that drives my efforts and the desire to learn day to day with the hope of retributing somehow all that it has give me.

Acknowledgements

Thank you...

To Professor Michael Bittner, Dr. Thomas Holzer-Popp and Dr. Marion Schroedter-Homscheidt for giving me this opportunity and their support.

To my colleagues Lars Klüser, Miriam Kosmale, Niels Killius and Dymitro Martinenko for their generous help and optimism.

To Dr. Detlev Heinemann for strengthening my interest in this field by his lectures and for his advisory. To Dr. Konrad Blum, Mr. Edu Knagge, Mr. Hans Holtorf, Dr. Elke Lorenz and all the PPRE staff for their interest and efforts in offering us the best experience in our program.

To Gisela Kanngießer and her daughter Leona for giving me a warm and familiar stay in Oldenburg.

To William Castillo and Maritza Sarmiento, my friends from the distance.

To Amjad Ayoubi and David Thamani, always nice partners in this experience. Thank you for encouraging me with your faith and joyful similes.

To DAAD, especially Mrs. Julia Hillman and the team of the Development Related Postgraduate Courses for their permanent attention and support from the beginning of this experience.

To all those have remembered me in their prayers.

Declaration

I state and declare that this thesis was prepared by me and that no means or sources have been used, except those, which I cited and listed in the Bibliography section. The thesis is in compliance with the rules of good practice in scientific research of Carl von Ossietzky University of Oldenburg.[a]

Diana Rocío Mancera Guevara

Oldenburg, 20^{th} of March 2013

[a] http://www.gremien.uni-oldenburg.de/download/good_scientific_practice_neu_10.05.2011pdf.pdf

Abstract

This study is intended to depict the presence of aerosols in the lowest portion of the Planet Boundary Layer in order to provide a starting point for those who aim to determine the influence of such particles in the energy production in CSP plants. A review of the State of the Art of the exploration of vertical profiles of aerosols is presented. By means of retrieval of remote sensing data from CALIPSO an outlook about the aerosols in the 150m above the ground is presented. Findings are discussed and some perspectives of the near future conclude the document.

Table of Contents

List of Figures

List of Tables

List of Abbreviations

ABC	Atmospheric Brown Clouds
ABSC	Attenuated Backscattering Coefficients
ACE	Atmospheric Chemical Effects
AERONET	AErosol RObotic NETwork
AFWA	Air Force Weather Agency (United States)
AMMA	African Monsoon Multidisciplinary Analysis
AOD	Aerosol Optical Depth
a.s.l	above sea level
BC	Black Carbon
BSC	Back Scattering Coefficient
CAD	Cloud Aerosol Discrimination
CALIOP	Cloud Aerosol LIDAR with Orthogonal Polarization
CALIPSO	Cloud-Aerosol LIDAR and infrared Pathfinder Satellite Observation
CAM	Community Atmospheres Model
CARMA	Community Aerosol and Radiation Model for Atmospheres
CPC	Condensation Particle Counter
CSI	Critical Success Index
CSP	Concentrated Solar Power

CTM	Chemistry Transport Model
DLR	Deutsches Zentrum fr Luft- und Raumfahrt (German Aerospace Center)
DMA	Differential Mobility Analizers
DMSP	Defense Meteorological Satellite Program
DREAM	Dust REgional Atmosphere Model
EARLINET	European Aerosol Research Lidar Network
EC	Elemental Carbon
ECMWF	European Centre from Medium-rangeWeather Forecasts
FAR	False Alarm Rate
FSSP	Forward Scattering Spectrometer Probe
GCOM-W1	Global Change Observation Mission Water
GFS	Global Forecasting System
GLAS	Geoscience Laser Altimeter System
HSRL	High Spectral Resolution LIDAR
IIR	Imaging Infrared Radiometer
IRENA	International Renewable ENergy Agency
LIDAR	LIght Detection And Ranging
LITE	LIDAR In-Space Technology Experiment
LFC	Linear Fresnel Collector
MAC	Maldives Autonomous Campaign
MM5	Mesoscale Meteorology Model
NAN	Not a Number
NCAR	National Center for Atmospheric Research (United States)
NCEP	National Center for Environmental Prediction (United States)
NIES	National Institute for Environmental Studies (Japan)
NWA	North-West Africa
OCO-2	Orbiting Carbon Observatory
OPC	Optical Particle Counter
PARASOL	Polarization & Anisotropy of Reflectances for Atmospheric

	Sciences coupled with Observations from a LIDAR
PBL	Planet Boundary Layer
PDF	Probability Distribution Function
POD	Probability of Detection
PRD	Pearl River Delta
PTC	Parabolic Trough Collector
PV	Photo-Voltaic
REACCESS	Risk of Energy Availablity:
	Common Corridors for Europe Supply Security
SAMUM	SAharan Mineral dUst experiMent
SCA	Scene Classifications Algorithms
SDS	Scientific Data Set
SMONEX	Summer Monsoon Experiment
SSA	Single Scattering Albedo
TOA	Top Of Atmosphere
TDR	Total Depolarization Ratio
TOMS	Total Ozone Mapping Spectrometer
UAV	Unmanned Aircraft Vehicle
VELIS	Vehicle Mounted LIDAR
VFM	Vertical Feature Mask
WA	West Africa
WFC	Wide-Field Camera

CHAPTER 1

Introduction

1.1 Motivation and context

Facing the compelling need of having energy alternatives to supply the world demand without jeopardizing the environment, renewable energy plays an increasingly important role in the development of the society and it is a particular issue of concern of technical and scientific circles. According to the last report of the *International Renewable Energy Agency*, by the end of 2011 the power generation capacity from renewable resources had risen to around 1 360GW. In spite of such capacity is distributed among a variety of technologies, solar technologies are achieving the highest percentages rates of growth. Although it is true that the largest portion of the aforementioned growth comes from the rise of PV (Photo-Voltaic) installations, CSP (Concentrated Solar Power) has also expanded at some extend. CSP total installed capacity at the end of 2011 reached 1 760MW and by October 2012 was around 2 400MW, most of which is currently concentrated in Spain and in the United States. However a growing number of countries including United Arab Emirates, India, Algeria, Australia, Morocco and Italy start to swell the list of investors in

CSP projects. CSP spans in turn different technical concepts and devices. Parabolic Trough Collectors (PTC), Linear Fresnel Collectors (LFC), Solar dishes and solar towers make part of the current markets offer. Despite PTC systems have predominated, solar tower technology could potentially achieve a larger share in the projects due to its superior capacity factor and accordingly higher efficiency[IRENA, 2012]. Every investment requires to know in advance the feasibility and the expected performance of the projected power plant. This includes the characterization of the solar irradiation, water availability and grid connectivity among others. The problem of the presence of aerosols in the atmosphere has not been properly described but for tower systems this knowledge might add some reliability to the assessment previous to the investment.

A sketch of the main components and arrangement of each mentioned technology is presented in the figure 1.1.

In solar tower technology, towers have a receiver mounted in its top part where the light is focused by mirrors called heliostats. These mirrors are located in the ground and by means of two axis movements they track the sun individually. The captured light is converted into heat to drive a thermodynamic cycle to generate electric power. The processes of absorption and scattering by air molecules, water vapor, aerosols and clouds are responsible for the generation of a diffuse component derived from the solar light. This diffuse portion along with a direct component makes up the total solar irradiation. CSP technologies take advantage of the direct component, which is highly affected by cloudiness. It explains why the best locations for CSP plants are those with low levels of cloud coverage.

The determination of the direct component hitting the surface requires knowledge of the influence of the atmosphere, by taking into account the distribution and effect of its components and the geometry and layout of the considered solar systems.

From the different components of the atmosphere that can influence the radiation transfer mainly the following groups have to be considered: clouds, the highly variable amounts of water vapor, aerosol particles and the gaseous molecules of dry air

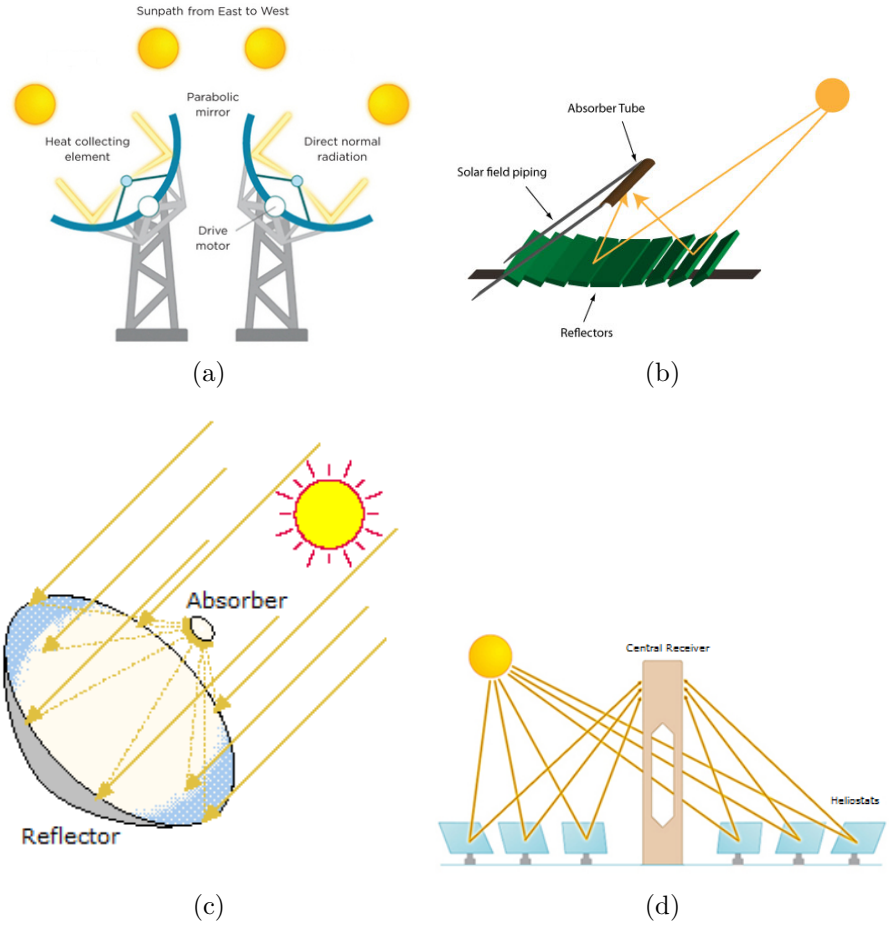

Figure 1.1: Parabolic Trough Collector (a). Linear FRESNEL Collector (b). Dish Collector (c). Solar Tower (d).

(Nitrogen, Oxygen, Argon, and traces of others), see table 2.1 [Heinemann, 2010]. Aerosols are defined as solid or liquid particles suspended in the atmosphere. They can arise either from natural sources like dust, sea spray and volcanoes, or from anthropogenic activities like soot, that is a result of incomplete combustion of fuels. Their sizes range typically between a few nanometers (nm) and tens of micrometers (μm).

In view of the influence of the atmospheric conditions on the running of solar systems, ambitious projects like DESERTEC and other new initiatives around the world that have CSP technology as a key element face not only economic but technical and scientific challenges to take the most advantage of the thermal properties of the sun radiation. One of them is to characterize the pronounced influences that different atmospheric agents exert in the systems' performance. In the specific case of solar tower technology, due to the large distances travelled by the sun's rays along their trajectory between the heliostats and the tower (at present, the height of solar towers is around 160m), the question arises to what extent the radiation is extinguished.

According to the report about the global scale technical potential of CSP presented in 2009 within the framework of the European project REACCESS (Risk of Energy Availablity: Common Corridors for Europe Supply Security), the total estimated potential of this technology is 2 945 926 TWh/y, expected from regions which ecosystems are predominantly desertic [Trieb et al., 2009]. Thus, issues like patterns and phenomena associated to aerosols including dust, turn relevant. The presence of the latter could change the expected energy yield due to extinction processes.

Faced with the mentioned circumstances it is necessary to describe as clearly as possible the atmospheric conditions under which tower systems have to operate. The geometric arrangement of a solar tower CSP installation leads to inquire about the horizontal and vertical distributions of particulate matter present in the surrounding air. Given the typical heights of towers, the first 200m above ground

become significant in the evaluation of the atmospheric conditions relevant for the operation and performance of this kind of systems.

The occurrence of atmospheric phenomena like wind circulation, turbulences and effects of convection, added to conditions like the roughness and the release of particles from ground and water surfaces and the emission of particles result of human activities leads to expect a high amount of aerosols in the near-surface layer. Then one more question arise, *is the presence of aerosols in the first 200m of altitude actually significant compared to that observed in a more extensive column of air?*

In order to get close to the answer of some of these issues and from the spectrum of measurement possibilities the present study makes use of the relatively unexplored potential of active remote-sensing to profile the vertical distribution in the lowest part of the Planet Boundary Layer (PBL).

Throughout this document the reader will be guided up to the results in a progressive way starting with a quick review of basic concepts that will be referred through the document, the state of the art of the estimation of aerosols in the lowest altitudes of the troposphere (the lowest portion of the Earth's atmosphere), and the assumptions and choices made in the treatment of satellite data to obtain the presented plots. A discussion of the results and some conclusions and recommendations close the document.

1.2 Objectives

As stated before the prior knowledge of the prevalent environmental conditions of a location where a CSP plant would be built is a key factor in the investment decision.

For tower systems the aerosol characterization is one of the aspects that needs to be clarified in advance. The traditional way would require long time and the use of expensive instruments. The use of remote sensing might contribute to achieve acceptable results with a fraction of the investment.

In this framework, this project aims to characterize the aerosols in the first vertical 150m above the ground based on satellite data. The limit of 150m was chosen

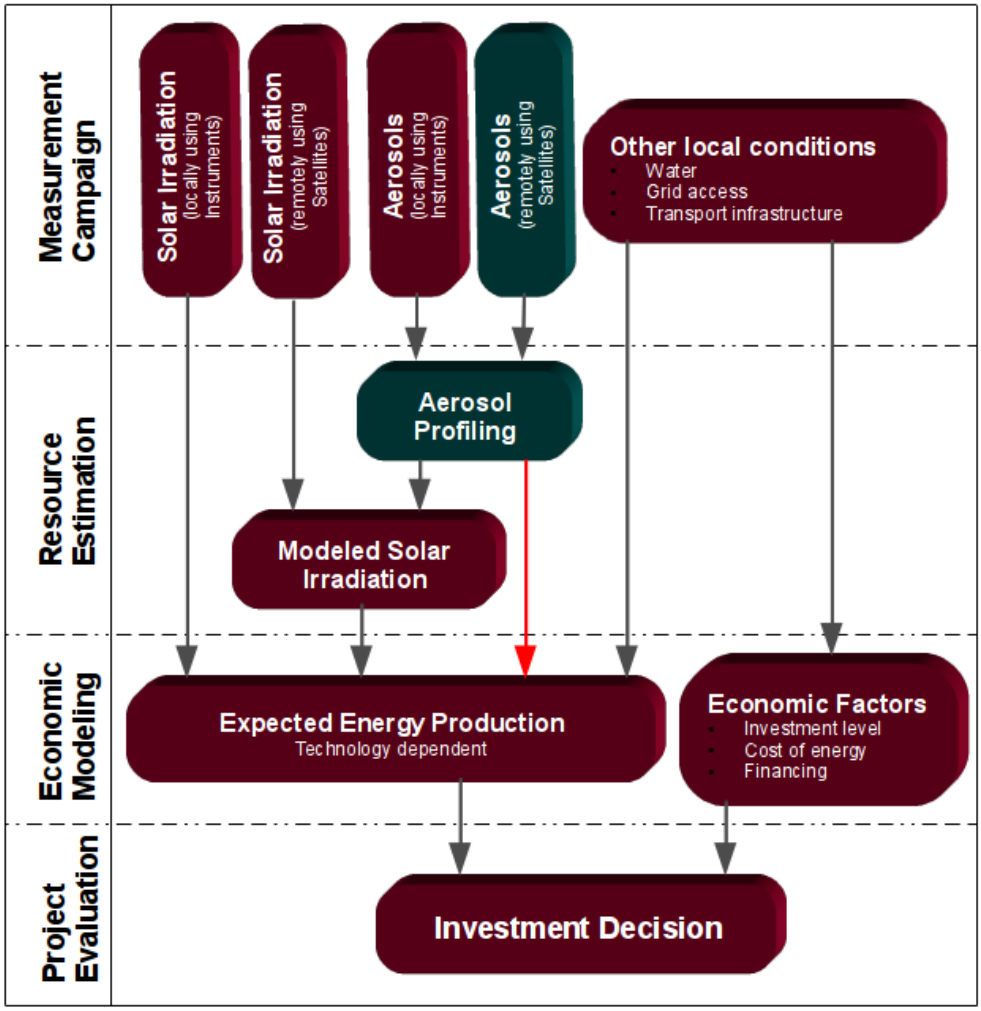

Figure 1.2: The phases of a typical investment decision in a CSP project. The first steps aim for the determination of the available resources, mainly the solar irradiation, which can be assessed either by local measurements or by satellite based prospection. The same applies to the aerosol profiling. One important remark is that the influence of aerosols in the operation of a CSP plant is an open question under research. Therefore the red arrow, meaning a non characterized relation. Due to this fact, currently the aerosols are seldom included in the evaluation of the energy models of CSP plants. Once the resources are estimated, an economic model is used to obtain the parameters later used to take the investment decision. The blocks in blue are covered in this work.

basically taking into account that the height of the current solar tower systems is in that order of magnitude. To mention two examples, Gemasolar Tower is 140 m high [Torresol_Energy, 2011], while Abengoa's PS20 is 165 m. [Abengoa, 2009]. Both plants are located near Seville, in Spain.

A review of the current state-of-the-art is the basis on which a further analysis of the light extinction could be realized. For that reason it was proposed as additional to present and contrast several techniques and measurement campaigns that aimed to profile vertical distribution of aerosols. Those experiences are accounted to support the decision on working with satellite data in the characterization of the light extinction at the selected height.

The parameter to describe such extinction along the vertical path of light is the Aerosol Optical Depth (AOD) obtained from the extinction coefficient. The source of data is the CALIOP module of the CALIPSO satellite. Climatology understood as the averaged conditions of weather and climate variables over a period of time was applied in this specific study for two years of data, 2007 and 2008. It is important to notice that only the total effect of the aerosols is taken into account, putting aside the discrimination of the type of particulate involved in the extinction processes, since for the CSP plant the relevant fact is the loss of energy, not who caused it.

Given the magnitude and importance of initiatives like DESERTEC and projects around the potential of the dessert regions of North Africa and certain zones of the countries that border the Mediterranean Sea, the selected area for the present study covers the region delimited by longitudes between 15°W and 40°E and the latitudes between 20°N and 45°N.

As a result, the maps of the AOD for the lowest averaged 150m, the one of the total AOD for a column of 8,2km of air and the corresponding ratio of AOD 150m respect to the latter for the aforementioned region are presented. The motivation to consider 8,2km as the total column of air has its roots in the occurrence of dust events (important contributors to light extinction) where particles can extend up to 7 or 8km besides technical reasons that as the 150m range will be further explained

in the section of Treatment of Satellite Data.

CHAPTER 2

Theoretical Basis

In general, remote sense techniques use as principle the interaction between radiant energy and the particles or environments to be analyzed. In the considered module CALIOP of CALIPSO satellite, laser light is used as diagnostic tool for atmospheric applications. The concept of these measurement techniques is based on measuring the characteristics of the scattered light and relating them to theoretical models of the underlying physical process[Witschas, 2012].

Different parameters and expressions of physical responses of the particles to the energy stimulus can provide information to characterize such particles and to describe the phenomena in which they are involved. For the case of light, the retrieval of optical properties plays an essential role in the understanding of the mentioned matters attributes and phenomena.

One of these parameters is the backscatter coefficient β that determines the strength of the LIDAR signal. It depends on the wavelength, the distance travelled by the light and the physical properties of the interaction between the light and the particles. This parameter describes how much light is scattered into the backward direction, for the case of LIDAR, in the direction of the receiver. It means, it is

the scattering coefficient for the scattering angle θ=180°. Since the laser light is scattered by air molecules (nitrogen and oxygen) and particulate matter, β can be defined as in Equation 2.1.

$$\beta\,(R,\lambda) = \beta_{mol}(R,\lambda) + \beta_{aer}(R,\lambda) \tag{2.1}$$

β : Total backscatter coefficient

β_{mol} : Molecular backscatter coefficient

β_{aer} : Aerosol backscatter coefficient

R : Distance travelled by the light

λ : Ligth wavelength

Molecular scattering mainly depends on air density. Then viewed from above from the downward looking systems of a spacecraft it increases with distance. On the other hand the scattering due to aerosol particulate is highly variable on spatial and temporal scales[Weitkamp, 2005]. The extinction coefficient commonly denoted by κ is the imaginary part of the index of refraction. It depicts how certain optical medium attenuates the radiation. The aerosol extinction coefficient is the sum of the aerosol scattering coefficient and the aerosol absorption coefficient. This parameter is expressed in terms of the inverse of length measurements (m^{-1}).

Contrary to water vapor, in which absorption represents nearly the total contribution to the extinction of the radiation, aerosols make the strongest contribution to the total extinction of the radiation by means of scattering processes in the visible range. The table 2.1 allows noticing the estimated shares of influence of both processes for different atmospheric constituents.

The Aerosol Optical Depth AOD is a dimensionless measure of how opaque the atmosphere becomes along a vertical trajectory of the light considering the aerosol influence. AOD is defined as the integral in the vertical axis of altitude of the aerosol extinction coefficient from the earth surface to the Top Of the Atmosphere (TOA)[Chung, 2012], as seen in equation 2.2.

	absorption	scattering
Ozone (O_3)	●	○
O_2, CO_2	●	○
Other air molecules	○	●●
Water Vapor	●●	○
Aerosols	●	●●
Clouds	●	●

Table 2.1: Contribution of atmospheric constituents to total extinction at visible wavelengths. (○= weak, ●= intermediate, ●●= strong) Source:[Heinemann, 2010].

$$AOD = \int_{GroundLevel}^{TOA} \kappa \cdot dz \tag{2.2}$$

AOD : Aerosol optical depth

κ : Extinction coefficient

dz : Heigth differential

Regarding identification processes, some types of particles can be inferred and described by means of the response to the incident radiation in three parameters retrieved from the returned signal:

1. Intensity: the intensity of backscattered radiation reveals the magnitude of the scattered light that allows characterizing the particles.

2. Frequency response: the frequency shift of scattered radiation corresponds to the difference between the initial and final molecular states, so allowing retrieval of parameters like temperature.

3. Polarization changes (changes in the orientation of oscillation plane of the electric field of the captured backscattered light respect to the orientation of the initially emitted beam).

Thereby, analysis of alterations in polarization allows the identification of particle features like the shape since whereas spherical scatterers do not change the

polarization state as response to linearly polarized laser light, non-spherical particles depolarize (change the direction of the electric field) the backscattered radiation. From this concept arises the parameter with which the sphericity of the particles is quantified: the linear depolarization ratio. The latter is defined as the ratio between the orthogonal and parallel planes of polarization of backscattered light. Those signals are detected via a beam splitter after a linearly polarized laser pulse is transmitted.

CHAPTER 3

State of the Art

In an endeavor to characterize in the best possible way aerosols and other particles along the vertical path of a column of air, different approaches have been implemented. In this study they are categorized in four classes: ground-based, airborne, satellite measurements and predictions coming from transport models. Some of the most currently employed instruments and some representative experiences all over the world will be referred throughout this section. Only limited cases have achieved relevant information about the lowest altitudes of the PBL, either because technical limitations or because it was not considered within the initial scope of the study.

3.1 Ground-based measurements

This sort of measurements facilitate the monitoring of specific local conditions as well as regional events of large scale because from several spatially spread stations it is possible to follow simultaneously the course of phenomena that usually evolve rapidly such as volcanic emissions. Fixed LIDARs, vehicle-mounted LIDARs, and nephelometers are part of the instruments that have been of the set of tools used to

profile vertically the atmospheric particulate.

3.1.1 Instruments

LIDAR

LIDAR is the acronym of LIght Detection And Ranging, it is nowadays a very powerful tool in remote sensing techniques that makes possible to profile the presence of different particular matter in the atmosphere (more commonly non-molecular elements). An special type of LIDAR, called Raman, can even derive water vapor profiles.

LIDAR has largely contributed to the knowledge of the Earths atmosphere since its first appearance back in the 1930's when pulses of light were used for the first time to measure cloud base heights. Later the acronym was introduced for this kind of technique by Middleton and Spilhaus in 1953.

In principle, a LIDAR consists of a transmitter and a receiver. Light pulses are sent into the atmosphere through the transmitter, they hit air molecules and other particles and light is scattered by them. The scattered light is sent into different directions and that backscattered is detected by the receiver. From the signals time delay and the speed of light (assuming vacuum) the distance where backscatter originates is determined. Different kinds of laser are used as transmitter and telescope optics plays the part of the receiver. Short light pulses with lengths of a few to several hundred nanoseconds and specific spectral properties are generated by the laser. Depending on the wavelength of the laser light used, LIDAR systems are more or less sensible to molecular or particle backscattering. At the receiver end, the telescope collects the photons backscattered from the atmosphere. It is usually followed by an optical analysing system which, depending on the application, selects specific wavelengths or polarization states out of the collected light. Then the received optical signal is converted into an electrical signal. In spite of its usefulness, its design has a limitation for ground-based measurements in the lowest layers. The so called incomplete overlap represents a limiting factor to the data reliability in

the closer distances to the emitted laser beam. The geometric arrangement of the emitter and receiver optics determines the degree of signal compression at distances close to the LIDAR. In the near-field range the laser beam cannot completely be imaged onto the detector. Thus, only a part of the actual LIDAR return signal is measured. This part varies with distance and depends on laser beam diameter, shape, and divergence, the telescopes imaging properties (focal length/diameter ratio), the receiver field of view and the location of emitter and receiver optical axes relative to each other. As it can be observed in the figure 3.1, the field of view of the receiver (gray) and the laser beam (area in which the beam is sent and it is expect to be back) (green) does not coincide for an initial segment starting at the device. This effect can considerably influence the vertical profiling up to several kilometres especially in the case of systems with a receiver characterized by a narrow field of view.

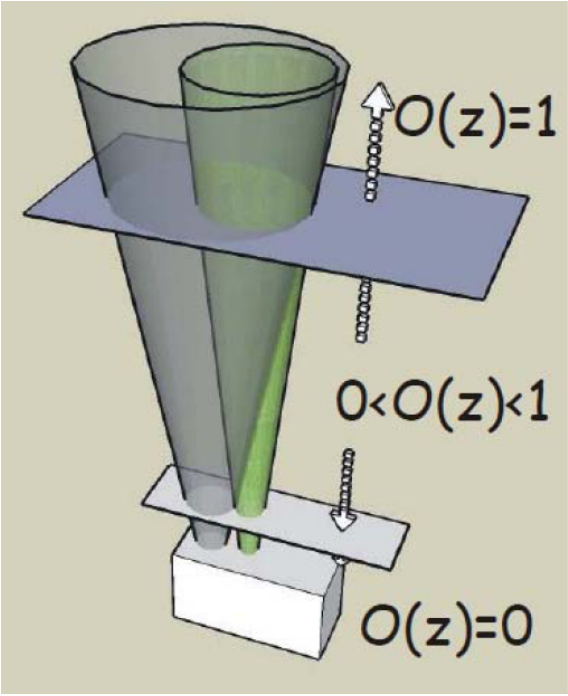

Figure 3.1: Incomplete overlap of the laser beam respect to the field-of-view of the receiver in a LIDAR. [Navas-Guzmán et al., 2011].

To approach the proper study of the lower layers of the atmosphere through ground-based LIDARs, several solutions have been used to solve this problem. One of the suggested methods is to apply a correction factor of the range-dependant

overlap characteristic, either analytically, by the application of a ray-tracing model or experimentally. However these techniques present important limitations because they require the knowledge of some technical parameters (usually not available) and the existence of homogeneous aerosol conditions, condition that can be seldom guaranteed in the lower altitudes [Navas-Guzmán et al., 2011]. Another option is to solve the problem by making use of the LIDAR's flexibility. LIDARs can be set up on aircrafts and satellites to overcome this problem and to offer more coverage for the lower layers of the atmosphere.

Nephelometer

This is an active instrument that measures the light scattered by the aerosol and subtracting light scattered by the gas, by the walls of the instrument and the background noise in the detector. Although it shares the principle of the LIDAR in the sense of it uses the detection of scattered light to characterize particles, nephelometer only considers air samples that it analyses locally, so that unlike LIDAR it is not able to provide spatial range profiles.

3.1.2 Experiences

The use of these tools either through campaigns or by means of permanent stations has contributed not only to evaluate their features of performance, reliability and limitations but also to continue the exploration of atmospheric matters properties and patterns. Some case studies of ground-based measurements made by different parties are referred below:

PAUR II

In the campaign PAUR-II (Photochemical Activity and Ultraviolet Radiation Modulation Factors) at Crete during spring 1999 it was explored the effect of a Saharan dust event due to transport over the Mediterranean area. This campaign was carried out by the operation of a VELIS (Vehicle Mounted LIDAR system) with a

two receiver configuration: one for the near range (100m - 3 000m) and the second one for the far range (1,5km - 25km). In spite of the possibility given by the near range LIDAR, in this project, observations were defined to start at 240m above sea level (a.s.l) with 5 minutes averages and with an available vertical resolution of 75m. From the collected values of the orthogonal and parallel components of the backscatter coefficient, LIDAR depolarization ratio was obtained ($D_a = \beta_{\perp a}/\beta_{\parallel a}$) for six different categories of aerosol particles, including PBL aerosols, thin-clouds from 2 to 5 km, desert dust, dust+water clouds, cirrus clouds and dust+cirrus clouds [Gobbi et al., 2000].

SAMUM 1 AND 2

As part of the project called Saharan Mineral Dust Experiment, these two campaigns were conducted during 2006 and 2008 in southern Morocco close to the Saharan desert and in Cape Verde correspondingly. A series of field observations made up of ground based, airborne and remote sensing had a strong focus on vertical profiling. To perform the ground based measurements three Raman LIDAR instruments of different spatial range were operated. However, the papers authors make a special remark regarding the missing information below 400m in the case of ground-based techniques. That lack is because measurements belonging to those altitudes are considered no reliable, due to the incomplete overlap of the laser beam to the receiver field of view.

PRD 2006

Since pollution in urban areas entails a serious problem in China, some campaigns were conducted at the Pearl River Delta (PRD), one of the most urbanized areas located in south-eastern China [Nishizawa et al., 2010]. The campaigns were carried out in autumn 2004 and summer 2006 with help of a dual-wavelength polarization Mie-scattering LIDAR developed by the National Institute for Environmental Studies (NIES, Japan). The aerosol vertical distribution was determined for the city of

Guangzhou producing as a result the plots presented in figures 3.2 and 3.3.

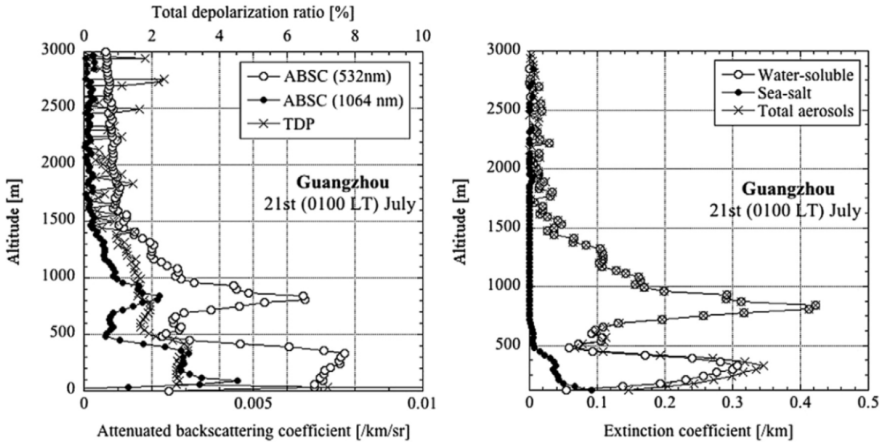

Figure 3.2: LEFT: Variation with altitude of attenuated backscattering coefficients (ABSC) for 532nm and 1064nm and total depolarization ratio (TDP) (%) for Guangzhou (left box). RIGHT: Variation of extinction coefficient with altitude in Guangzhou for water-soluble, sea-salt and total aerosols particles. [Nishizawa et al., 2010].

Likewise, figure 3.4 represents the results for Beijing. Those depict the different parameters for that city extracted from data collected there from 16 to 20 August 2010.

As can be observed the results revealed in the heights from 0 to 3km a day/night-time and spatial variation of aerosols and the dominant presence of water-soluble particles (like sulphate, nitrate and organic carbon particles) most of them being anthropogenic aerosols.

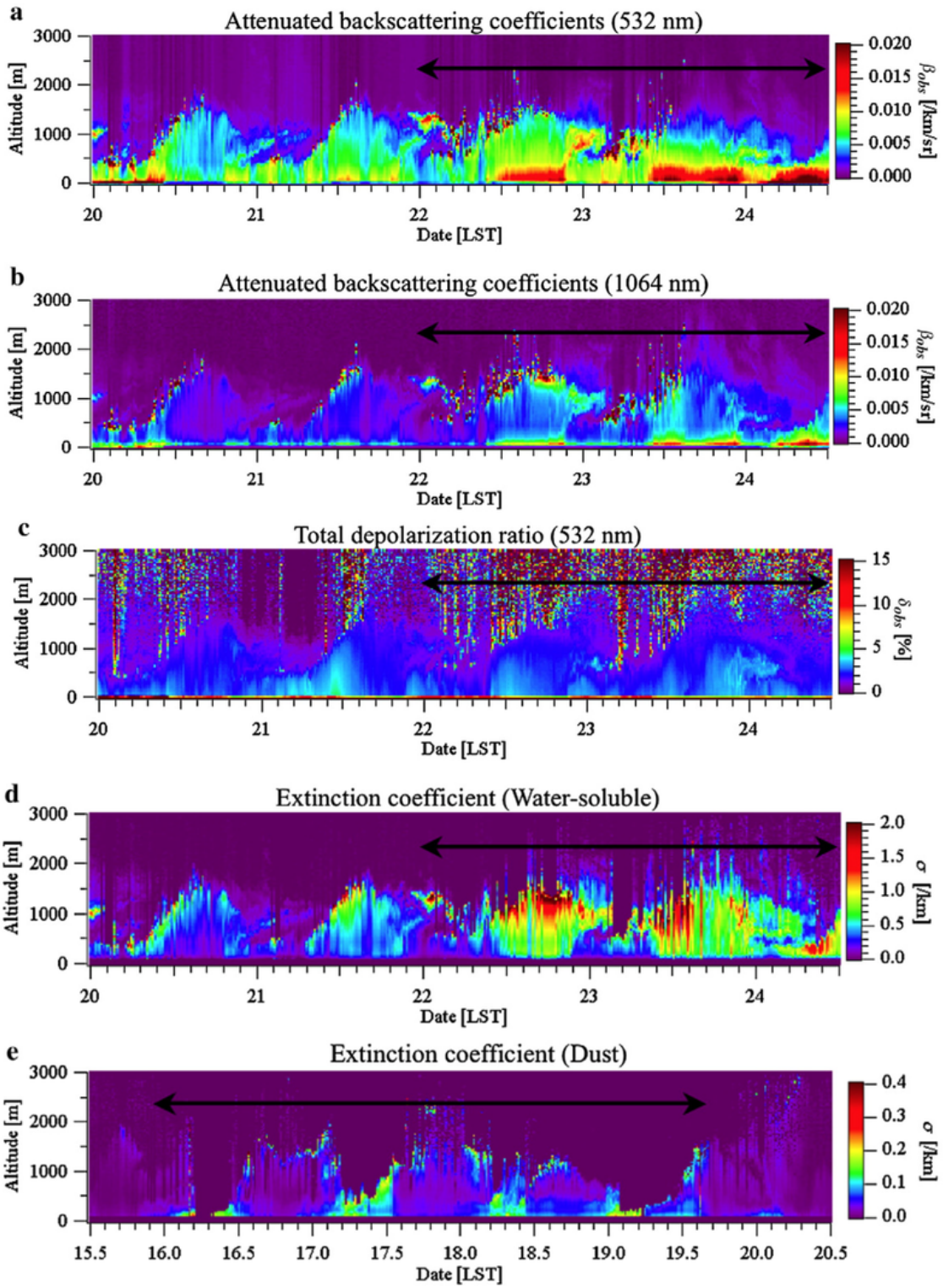

Figure 3.3: Temporal variation vs. height of: attenuated scattering coefficients at 532nm and 1064nm, (a and b), total depolarization ratio at 532nm (c), extinction coefficient of water-soluble asnd dust particles (d and e). Values for the Chinese city of Guangzhou. LST stands for Lunar Standard Time. [Nishizawa et al., 2010].

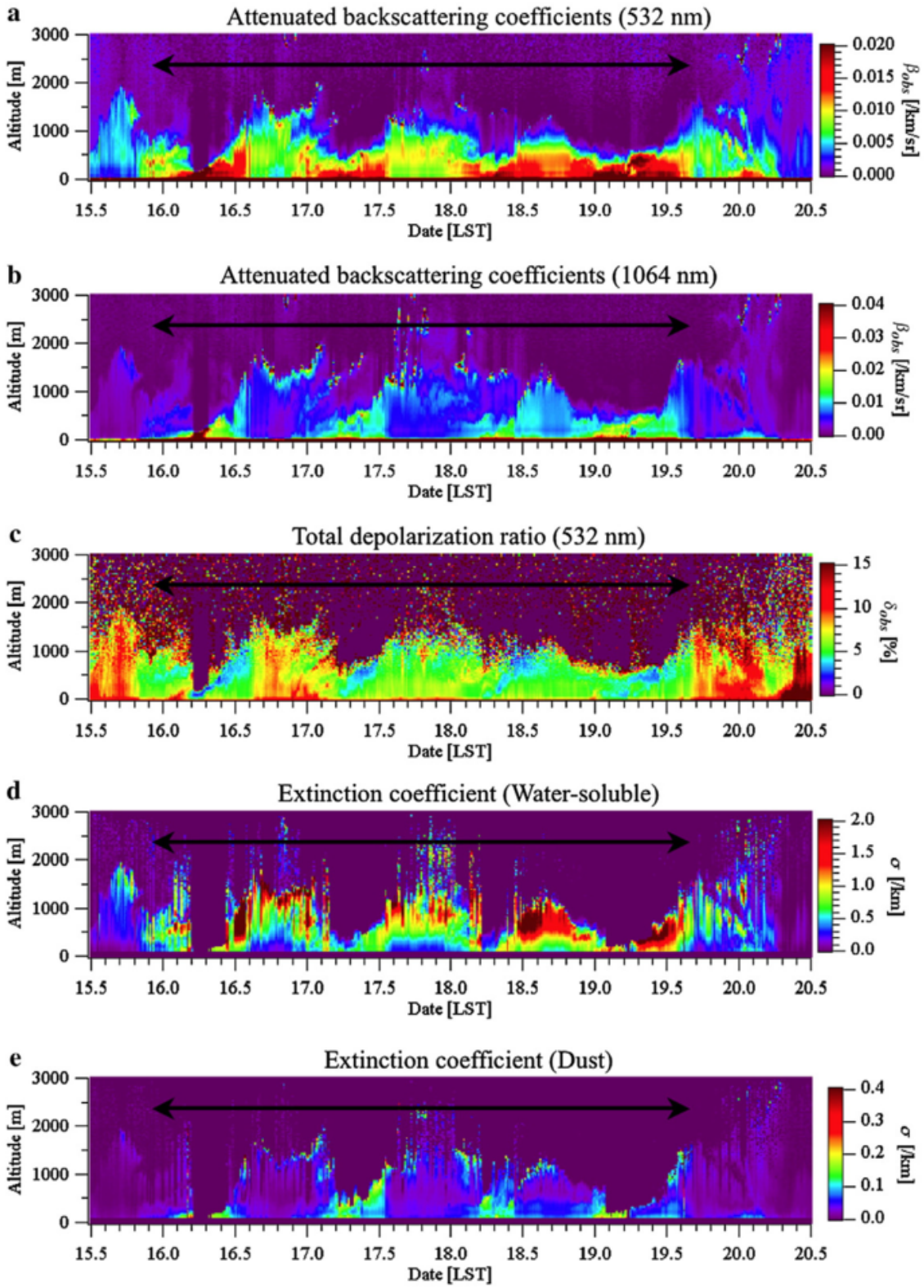

Figure 3.4: Temporal variation vs. height of: attenuated scattering coefficients at 532nm and 1064nm (a and b), total depolarization ratio at 532nm (c), extinction coefficient of water-soluble asnd dust particles (d and e). Values for the Chinese city of Beijing. LST stands for Lunar Standard Time. [Nishizawa et al., 2010].

EARLINET

The European Aerosol Research Lidar Network to Establish an Aerosol Climatology is a continental scale project that aims to provide quantitative, statistically relevant data set of the vertical aerosol distribution over Europe. The newtork is comprised by 15 stations located in 11 countries. The ground-based LIDARs in the different stations are the main tools that with help of data retrieved from instruments like sun photometers and satellite data have provided among others information about vertical and horizontal distribution of saharan dust observed over Europe, diurnal cycles, detection of aerosols emmited by forest fires and volcanic dust. However, even when several studies were aimed to depict phenomena in the PBL, the full overlap is not reached up to 300m to 500m in most cases. It means that depending on the case either the signal needs to be corrected or it can not be taken into account as reliable in the lowest part [Bösenberg and Matthias, 2003].

3.2 Airborne measurements

Both unmanned and manned aircrafts have been used as support and transport vehicles for payloads comprised by a variety of devices that can profile vertical structures of atmospheric particulate.

3.2.1 Instruments

A variety of physical principles have been applied to create measurement techniques and devices. Among those one can find LIDAR's, aethalometers, Differential Mobility Analizers (DMA), Optical and Condensation Particle Counters (OPC and CPC correspondingly). A quick view of some of them can be found below:

Aethalometer

The aethalometer^{TM} is an instrument that provides real-time continuous readouts of the concentration of black or elemental carbon aerosol particles (BC or EC) in

an air stream. These particles commonly called soot are emitted from all types of combustion, most notably from diesel exhaust[a]. The Aethalometer collects samples in a fiber tape and then it accomplishes an optical analysis of the blackness of the sample. The analysis of one measurement can take between 1 and 5 minutes.

Optical Particle Counter (OPC)

In general, the principle of a particle counter is counting the light pulses by scattered particles after those were placed in a chamber crossed by a laser, that is, sampling the air intended to be measured. Then the bounced flashes product of the scattering are received by an electrical device sensitive to light and are converted in digital pulses (small pulses for small particles, and larger signals for larger particles). Thus, information about size and quantity is decoded by the digital analyser placed in the last stage.

Condensation Particle Counter (CPC)

All the automated particle count techniques are limited by the smallest particle size that they are able to detect and the largest particle sizes determined by aerodynamics and inlet size. When particles become so small that the signal from them is comparable to the background noise, it is not possible to acquire reliable information. The solution proposed through CPCs is to make larger these particles so that they can be distinguished from the background noise. The CPCs have a tank that contains a volatile liquid. The samples of air are forced to flow through a warm chamber where it is mixed with the liquid vapour. Then the mix is moved to a cold chamber producing the supersaturation of the vapour and as a result the condensation over the particles. Thus, particles of up to $0{,}01\mu m$ are surrounded by vapour increasing their size up to 1 or $2\mu m$. The latter can now be easily detected. This method works mainly for hygroscopic / hygrophilic particles. Therefore for most desert dust particles this method is not reliable.

[a] `http://www.esrl.noaa.gov/gmd/obop/mlo/programs/esrl/aeth/pub/pub_magee_aeth.doc`

Differential Mobility Analyzer (DMA)

The Differential Mobility Analyzer is one of the most commonly used devices for classifying and measuring nanometer sized aerosol particles with diameters between 1nm to $1\mu m$ [Intra and Tippayawong, 2008]. In its typical geometry, this device is made up an assembly of two concentric cylindrical electrodes with an air gap between the walls (see figure 3.5).

In a first step the air and the aerosols contained in it are exposed to beta radiation in order to provide them with an electric charge which final value will depend on the size of each kind of particle. Subsequently the charged particles are introduced at the top of the cylinder and they flow passing along the annulus. Between the electrodes an electric potential is applied. While particles with high electrical mobility are collected on the upper portion of the rod, those with a low electrical mobility are collected on the lower portion and the particles with certain narrow mobility are led to the monodisperse slit located at bottom of the collector rod.

In this way they are separated by type and can be displaced to a device like a particle counter in order to determine their concentration per volume among other parameters that can be defined by means of chemical analysis. It is important to notice that this device could not be suitable to measure particles like desert dust close to the sources because they are in the range of 2μm to 20μm (effective diameter) [Ryder et al., 2012].

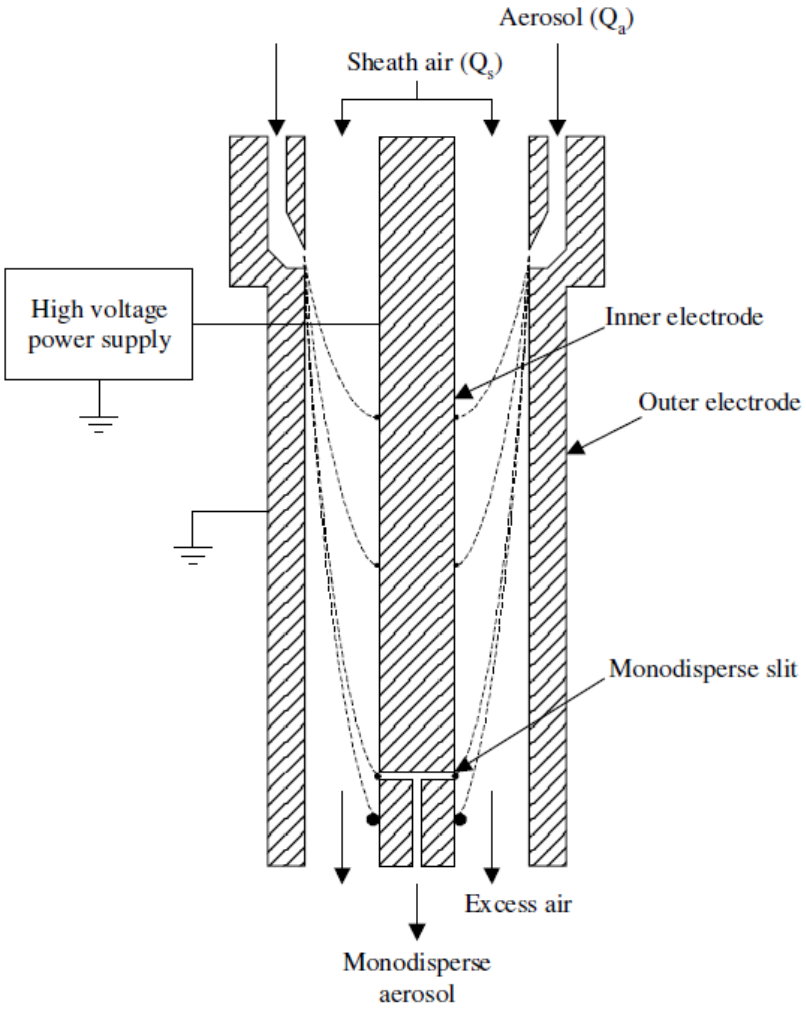

Figure 3.5: Sketch of the mechanism of a DMA. [Intra and Tippayawong, 2008].

3.2.2 Experiences

Some representative experiences which principle was based on aircrafts from different technical approaches are presented in the next sections.

Maldives Autonomous Campaign (MAC)

Preceded by the ABC project, this study [Ramanathan, 2006] conducted in March 2006 made use of a fleet of six UAVs (Unmanned Aircraft Vehicle) - figure 3.6. The launch done from the Maldives intended to scan the pollution (black carbon) coming from South Asia and dust from Arabian and South-Western Asian deserts, as well

Figure 3.6: Fleet of UAVs used in MAC campaign. [Ramanathan, 2006].

as their influence in clouds over an area of the Indian Ocean.

Measurements were made within the PBL. Even though the aerosol read-outs started as soon as the aircrafts took off, the black carbon measurements were taken only when certain height was reached. By means of a Condensation Particle Counter the plots presented in figure 3.7 were obtained.

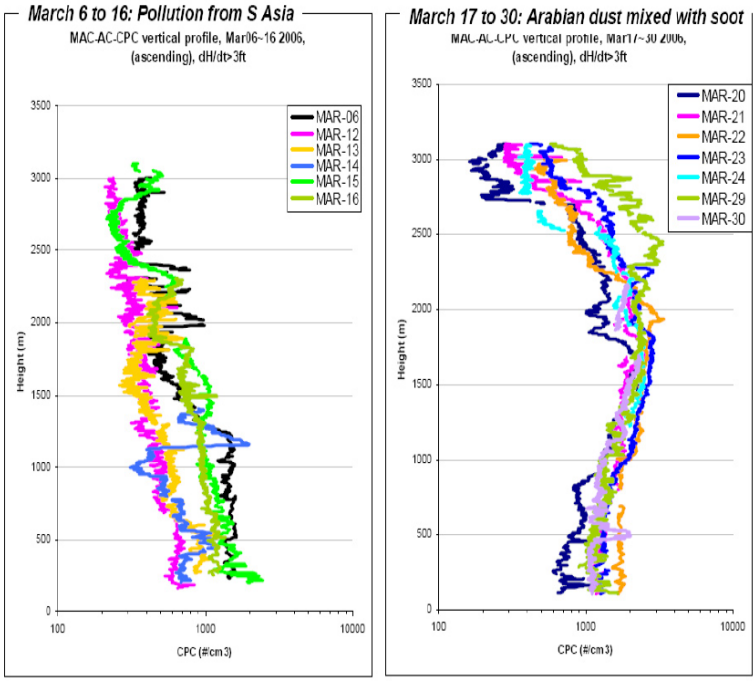

Figure 3.7: Results of measurements made with help of a CPC of pollution from South Asia around Maldives (LEFT) and the dust mixed with soot over the same region from Arabian deserts (RIGHT). [Ramanathan, 2006].

Summer Monsoon Experiment (SMONEX)

Through a series of research aircraft flights were conducted during spring and summer 1979 over Saudi Arabian Peninsula in order to collect useful information to document the radiation energy budget [Ackerman and Cox, 1982].

The aerosol vertical profiles provide information from 0km to roughly 7km. The figure 3.8 describes the variation of particle concentration (given in number per cm^3) as function of height through the data collected during four flights for three particle size ranges in accordance with the indicated convention. Here it is noticed that particle concentration decreases with height.

On the other hand, figure 3.9 depicts the dust mass loading given in $\mu g/m^3$ as function of height. This curve was obtained through the measurements of the number of particles per unit of volume acquired from the FSSP (Forward Scattering Spectrometer Probe) and the previous definition of this dust mass loading assuming spherical particles.

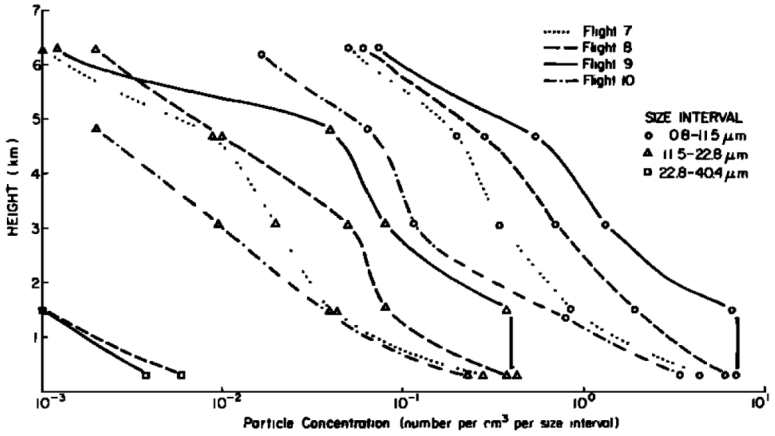

Figure 3.8: Particle concentration of three size ranges for flights 7 to 10 conducted during SMONEX campaign. [Ackerman and Cox, 1982].

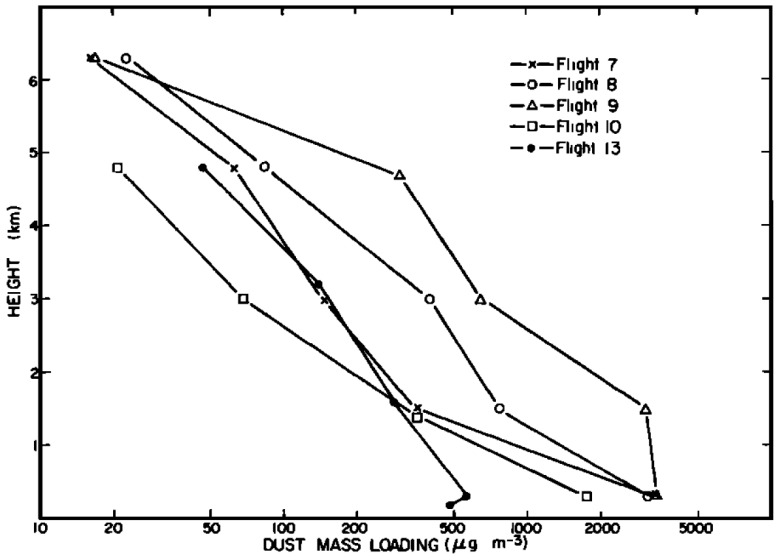

Figure 3.9: Dust mass loading ($\mu g/m^3$) as a function of height for various flights. [Ackerman and Cox, 1982].

SAMUM 1 AND 2

The project also mentioned in the ground-based measurements section tackled the task of scanning of the vertical profiles of the atmosphere by means of the use of the instruments of the payload onboard of the FALCON (figure 3.10), the aircraft of the German Aerospace Center (DLR). The main instruments of the payload were a High Spectral Resolution LIDAR (HSRL), a CPC and a DMA. [Knippertz et al., 2011].

Figure 3.10: Dassault Falcon 20E used for atmospheric research at DLR.

The graphs shown in figure 3.11 were obtained from the measurements of the HSRL over the Santiago and Fogo Islands in Cape Verde. The colour-coded images

show the ratio of total (particles+molecules) to pure molecular backscatter. Starting from the unity (light blue: particle free atmosphere), the values rise in the coloured bar as long as the aerosol load increases. By means of these measurements and due to their relatively low spatial variation, those obtained from the ground instruments were validated and described as representative.

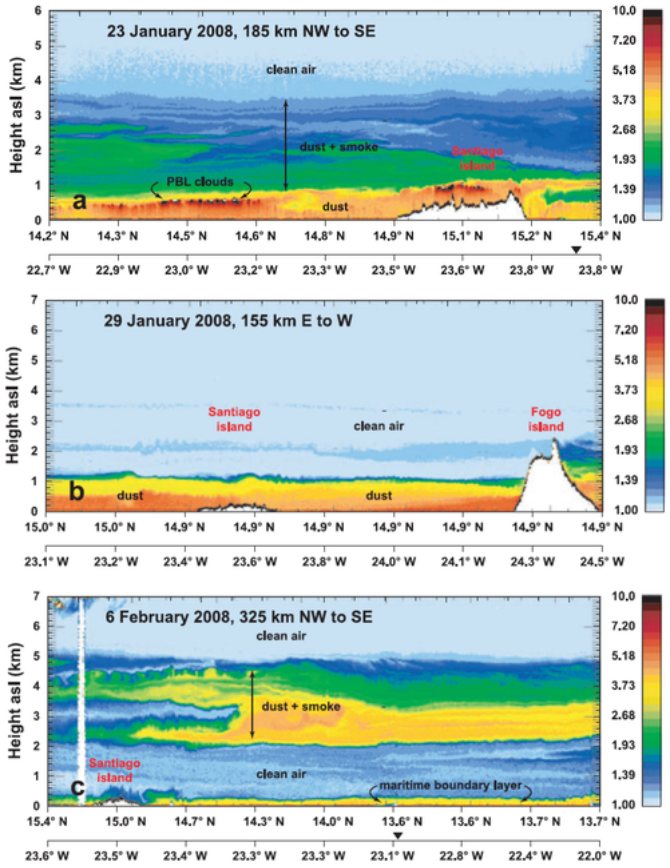

Figure 3.11: Results from SAMUM 1 and 2 campaigns for 23 and 29 January and 6 February 2008. Measurements of the depolarization ratio as function of height obtained from HSRL in the indicated zones. [Knippertz et al., 2011].

SAMUM Dakar

In the frame of SAMUM project a series of measurements were carried out over Dakar, Senegal.[Petzold et al., 2011]. The mixing of urban pollution with dust was studied through some tools that included airborne in situ instruments and an HSRL (the same used in SAMUM 1 and 2) aboard the Falcon aircraft. In this case, the experimental approach allowed a variation of flight altitudes from 900m to 9km a.s.l. The latter allowed obtaining vertical information between 0km and 2km a.s.l. as

shown in figure 3.12.

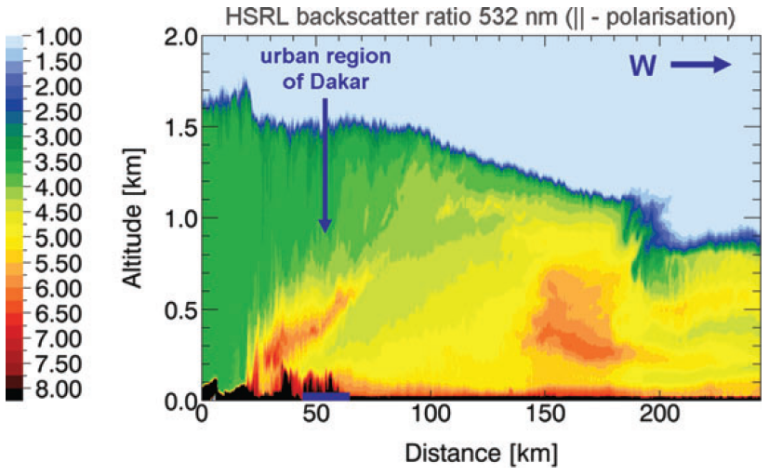

Figure 3.12: Backscatter ratio at 532nm vs. Height taken from an HSRL during SAMUM Dakar. [Petzold et al., 2011].

3.3 Satellite measurements

In contrast to ground-based systems, satellite techniques are able to provide near-global homogeneous coverage due to the orbit and the uniformity in format data. With nadir-viewing instruments, satellite provides a solution for the overlap function problem in the near-ground altitudes. Passive satellite techniques like imagery instruments (for instance MODIS) provide totalized values in the vertical range. They are not able to split the profiles in segments to analyze separated layers. Because of the aforementioned reasons among others, satellite measurements have gained importance. A general view of the most relevant instrument for this case and a reference experience will be provided below.

3.3.1 Instruments

Speaking of satellite alternatives to outline the vertical profiles of atmospheric constituents the most recent and still active tool is CALIPSO. Nonetheless before getting started with the review of this satellite it is worth to make a short mention of its immediate predecessor, the Geoscience Laser Altimeter System (GLAS) which

goal was to perform cloud top and height of the PBL determinations, as well as the first attempt in the space field, the LIDAR In-Space Technology Experiment (LITE). The latter was the first spaceborne LIDAR using Shuttle for 11-day flight. They were launched in 2003 and 1994 respectively.

Cloud-Aerosol LIDAR and Infrared Pathfinder Satellite Observations

CALIPSO (see figure 3.13) is an US-French satellite mission that has been in operation since April 2006. CALIPSO is part of the A-train (Afternoon Constellation) which six current satellites closely follow one after another (seconds to minutes to each other) along the same polar orbital track so that the near-simultaneous observations of the instruments aboard of them complement each other to provide a wider panorama of weather and climate change. Along with the already in orbit satellites Aqua, CloudSat, PARASOL, Aura, GCOM-W1 and the shortly part of the group OCO-2, CALIPSO provides data that have expanded the understanding of the Earths atmosphere and climate. CALIPSO is able to do measurements during both day and night in order to shape the vertical profile of clouds and aerosols distribution on a global scale, providing a new insight of the role that they play in the weather, climate and in the air quality. CALIPSO payload is comprised by three nadir-viewing instruments, as seen in figure 3.13.

CALIOP Cloud Aerosol LIDAR with Orthogonal Polarization is an airborne LIDAR operating in a satellite in orbit since 2006. The solid-state diode of CALIOP produces linearly-polarized pulses of light at two wavelengths (1064nm and 532nm). With two wavelengths it is possible to have interaction with a wider range of particle sizes, so that several types can be distinguished. The atmospheric return is collected by a telescope which in turn feeds a three channel receiver with the following information:

- The backscattered intensity at 532 and 1064nm.
- Parallel component to the polarization plane of the transmitted beam at 532nm.

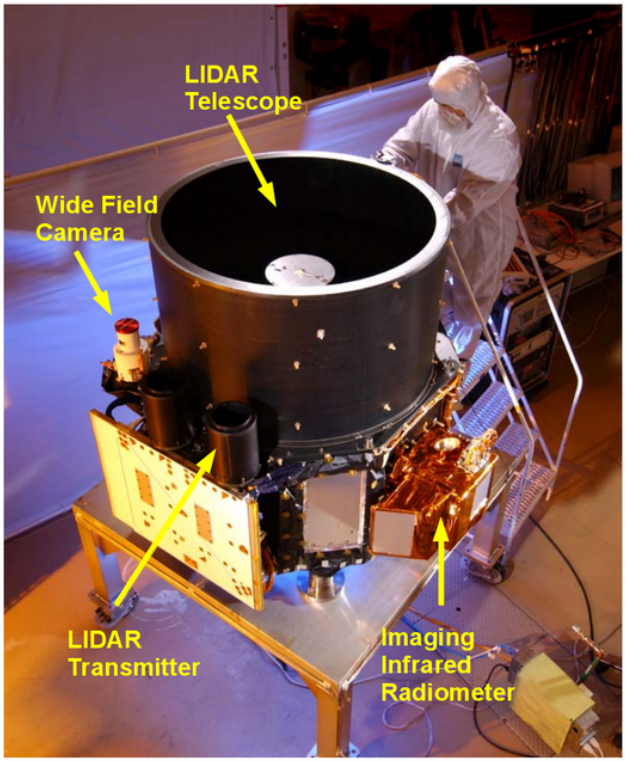

Figure 3.13: View of CALIPSO instruments. [Winker, 2006].

- Perpendicular component to the polarization plane of the transmitted beam at 532nm.

Thereby the LIDAR provides information useful in the determination of the vertical distribution of aerosols and clouds and their optical and physical properties (aerosol size, hydration, cloud water/ice phase, among others).

Some of the most relevant operational parameters of the CALIOP module are:

- Pulse Rate: 20,25 Hz
- Vertical resolution: 30m-60m (from -0,5km to 40 km altitude)
- Horizontal resolution: 333m
- Repeat Orbital Cycle: 16 days. Period after which the satellite crosses exactly the same point.
- Sun-synchronous orbit.

CALIOP is the only module of CALIPSO that provides direct information about vertical profiles.

IIR Imaging Infrared Radiometer, it is a detector of infrared radiation whose resulting measurements are processed to create an image. The instrument uses a microbolometer detector array that is a device for measuring the power of incident electromagnetic radiation. That radiation strikes the detector material, heating and through the changes of temperature the incident radiation is retrieved. The IIR has three channels in the thermal infra-red window region (8.65μm, 10.6μm, 12.05μm).

WFC Wide-Field Camera, it is a nadir-viewing instrument in the band 620-670 nm with a single channel that when combined with IIR module provides a wider context to interpret the LIDAR data.

3.3.2 Experiences

As illustrative example of CALIPSO data analysis the case of ABC project can be mentioned with the following annotations:

Atmospheric Brown Clouds (ABC)

Project ABC [Ramanathan et al., 2008] undertook the assessment of the impacts of ABC on regional radiative forcing, climate, agriculture, water and health in the Indo-Asia-Pacific region. Among other tools used to characterize the distribution of brown clouds (widespread layers of brownish haze consisting of mainly aerosol particles, such as black carbon (BC), and precursor gases which produce aerosols and ozone) is CALIPSO through which the vertical profile of ABC and dust is colour-coded. Measurements were conducted during 4 months of the dry season. Some of the results are illustrated by means of the figure 3.14.

In the colour-coded graphs measured at 532nm provided by CALIPSO each profile corresponds to the indicated date, covering the trajectory showed in the right

boxes. Information is given for altitudes from 0km to 10km. As observed, major contributions are roughly between 0km and 3km of altitude. Aerosols are represented by the green, yellow and red colours (low, medium and large backscattering). Boundary layer clouds usually shows up gray or white. Cirrus register colours from yellow to gray.

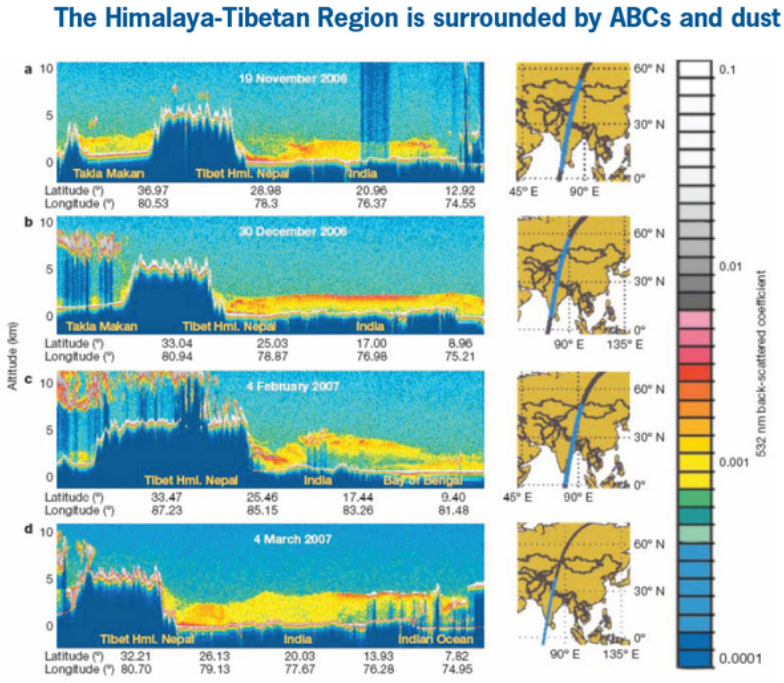

Figure 3.14: Colour-coded vertical profile of ABC and dust in the Himalaya-Tibetan Region taken by CALIPSO as part of ABC project.[Ramanathan et al., 2008].

3.4 Results from predictions of models

Under the context of atmospheric science a model can be defined in general as a mathematical formulation that describes a physical phenomenon. An example could be the temporal and spatial evolution atmospheric components such as aerosols on some of the associated processes to them (emission, transport, deposition, radiative influences, removal cycles etc) to obtain a prediction of its future state. However numeric prediction is largely a problem of initial conditions. For instance dust transport models have to be driven by some inputs like meteorological variables that play a role in the modeled process. Variables like wind speeds, moisture and

temperature can be required and those are provided by data assimilation (systematic and successive input of data) either from direct observations of the required variables or from values obtained by means of predictions of meteorological models. It means that two or more models might have to be coupled and modified if necessary. Some of the models and various applied cases are also presented.

3.4.1 CARMA

Community Aerosol and Radiation Model for Atmospheres was originally a one dimensional physical-chemical sulphate aerosol code developed with support of AFWA (United States Air Force Weather Agency) by Turco and Toon in 1979. Although the first version of simulation extended from the surface to an altitude of 58km, the tropospheric aerosol chemistry and physics were not fully analysed at that time therefore it was considered mainly stratospheric [Turco et al., 1979].

Reforms were subsequently introduced in order to raise the number of dimensions to 3 and to expand the model to four types of aerosols, including soil dust [Toon et al., 1988].

Its flexibility and a considerable number of updates developed since then allow that currently this model is often used as an interactive subroutine of regional dynamical models.

Some of the experiences with CARMA are:

CARMA case study I: Numerical simulations of asian dust and pollution. Atmospheric Chemical Effects ACE-ASIA (Su-Toon model)

A three-dimensional coupled microphysical/climate model was developed to investigate the sources, removal processes, transport and optical properties of Asian dust aerosol on downwind regions [Su and Toon, 2009]. The time frame of the model simulations was March-May 2001, the period corresponding to ACE-Asia experiment observations. The new numerical model combines the three-dimensional climate model CAM3 (Community Atmospheres Model) with the aerosol model CARMA2.3.

They also incorporated the Ginoux et.al [2001] function as dust source. The whole model is driven by assimilated meteorology from NCEP/NCAR (National Center for Environmental Prediction/National Center for Atmospheric Research). The coupled CAM3/CARMA2.3 spans 40km from the surface through 28 vertical model layers.

For comparison of modelled dust, vertical distributed LIDAR measurements were used. The data came from the NIES LIDAR in Japan which operates in Japan and China producing as a result a set of vertical profiles of backscattering intensity and depolarization ratio recorded every 15 minutes at a wavelength of 532nm. The goal by doing such kind of comparison was to check the effectiveness of the model to foresee the occurrence of dust including the agreement in the altitude factor. The study did not aim to compare the magnitude of the backscatter because due to the assumption of spherical particles during modelling a large unknown correction would be needed (dust particles are not spheres). The figure 3.15 depicts the BSC (Back Scattering Coefficient) derived from NIES LIDAR for April 2011 contributed by dust particles in Beijing (top) and the corresponding total dust mass density from Su-Toon model over Beijing (2 in the middle) and upwind Beijing (bottom) for the specified time.

In summary, for the Beijing case the model reproduced almost all the events during the period April 2001. Those are the following:

- Dust event on 2^{nd} April.
- Dust event on 4^{th} April.
- Dust event from 7^{th} to 8^{th} April.
- Event on 18^{th} April.
- Event on 28^{th} April.

However the model missed the following:

- Dust event on 10^{th} April (although there is a large dust mass density on that day located by the model in upwind of Beijing area).

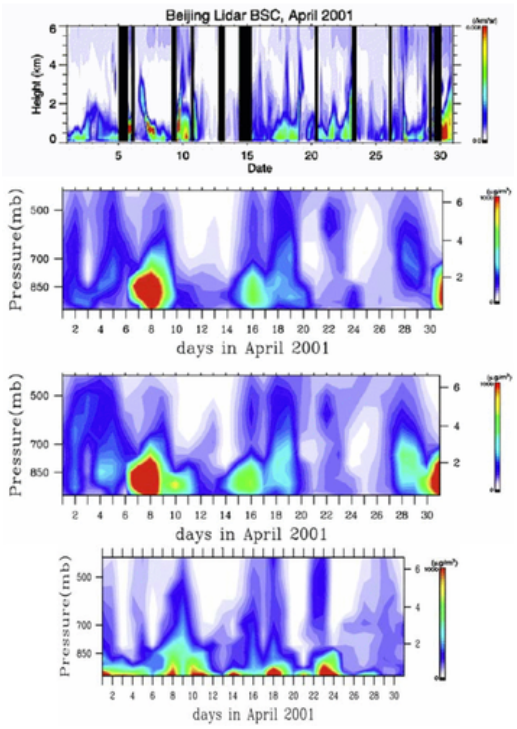

Figure 3.15: Results of dust analysis during April from NIES LIDAR (top) and from Su-Toon numerical model for vertical dust profile for Beijing area (over Beijing: second graph, upwind Beijing: third graph, North Beijing: bottom. [Su and Toon, 2009].

- The low-level loads occurred between 20^{th} to 24^{th} April (although according to the model they went to the north).

Regarding Nagasaki results (figure 3.16), the model generally well reproduced the following vertical distributions:

- Event on 12^{th}, 13^{th} and 14^{th} April 2001.

- Dust on 2^{nd}, 23^{th}, 26^{th} and 27^{th} April 2001 (but mainly in the free troposphere). The absence of dust on 26^{th} and 27^{th} April in the lowest layer is attributed according to the authors to wet deposition which in accordance to the model washed out the low level dust on the indicated dates.

Besides the failure in the 26^{th} and 27^{th} April events in the PBL, the model did not predict the dust load on 20^{th} April. This discrepancy is ascribed to incorrect modelled winds.

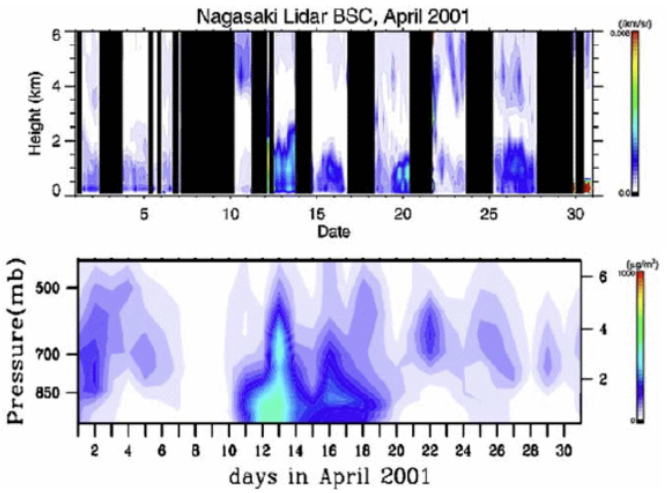

Figure 3.16: Images of LIDAR results (top) and model simulation (bottom) of Nagasaki area. [Su and Toon, 2009].

Although the model was worthy of a general good opinion from the authors, they think that further work is needed on the wet deposition process of the model to be more accurate near the surface.

CARMA case study II: Forecasting dust storms using CARMA and MM5 (Barnum)

CARMA model was modified by Johns Hopkins Applied Physics Laboratory in U.S.A to make daily dust forecasting by assimilating data from MM5 (Mesoscale Meteorology Model) weather model. The effectiveness of this coupled model to make forecast of dust events occurrence is evaluated by [Barnum et al., 2004]. For a 60 day period beginning February 15^{th} 2002 the study determined for Saharan Africa and Southwest Asia regions the forecast output of dust loading. It used satellite and ground based observations of dust events to determine by means of an observational method the presence or absence of them. The satellite imagery was extracted from DMSP (Defense Meteorological Satellite Program). Separate teams prepared and analysed the model results and the observation data to reduce possible human biases in the model evaluation.

The dust model outputs are total dust concentration in form of coloured maps at the selected altitudes by user and vertical concentration profiles for each 3 hours

period during 72 forecast hours. In this coupled model 18 out of 22 vertical levels are used between the surface and the 500mbar pressure level (5,6km) in order to optimize vertical resolution in the PBL. Deposition processes are described within this version of CARMA based on spherical geometry of particles. The model incorporates the global dust source data base developed by [Ginoux et al., 2001].

The skill scores used to evaluate the models effectiveness were the following:

- POD (Probability of detection)
- FAR (False Alarm Rate)
- CSI (Critical Success Index)

Because skill scores assessment purposes, the mesoscale is grouped into distinct regions. The model evaluation results show that Yemen and Oman have the lowest CSI where POD were only 19%. Authors of the mentioned study have dismissed the precipitation as the cause of the low forecast skill scores due to the low rate of precipitation over this region during the observations.

The authors attribute the cause of the low forecast skill scores to the weak representation of dust in the Ginoux source database in that region. Ginoux model was developed with help of TOMS (Total Ozone Mapping Spectrometer) satellite data [Ginoux et al., 2001] and it was evaluated by comparing its results with data coming from LITE. TOMS in turn is more sensitive to higher altitude dust concentration. This is because TOMS AI (TOMS Aerosol Index) is more sensitive to small airborne particles than larger sand particles near the surface. Thus, in the case of Yemen and Oman the POD of 19% can be explained because this regions produces surface-level dust event that have typically lower TOMS AI because the mentioned insensitivity in the lowest layer. According to previous studies, TOMS is least sensitive to aerosols in the boundary layer. Thus aerosols below ≈500-1000m are unlikely to be detected by TOMS [Prospero et al., 2002].

The authors noticed as well that the longer the forecast period, the larger the error and since the factor dust-source remains constant along the analysis, it led

them to think that under these timeline conditions MM5 weather model output wind speeds (dynamic in the time-line) can be the source of error that influences direct and negatively the dust forecast ability of the model.

In general from the qualitative analysis the authors have described the adaptation of CARMA and MM5 models as successful, showing to have good skill over Saharan African theater and South-western Asia.

3.4.2 CHIMERE

This is a dust dedicated offline modelling tool which allows performing multi-annual simulations with a relevant spatial and temporal scale. This model requires several meteorological variables as input such as wind temperature, mixing ratio for water vapour and liquid water in clouds, surface heat and moisture fluxes and precipitation. These meteorological fields can be taken from different meteorological models [Hodzic et al., 2004]. The emissions scheme used in the model is based on the Schmechtig, Marticorena and Bergametti's [1995] dust production mode [Vuolo et al., 2009].

CHIMERE-DUST case study I: Simulation of the mineral dust content over Western Africa from the event to the annual scale with CHIMERE-DUST model

In this study the Chemistry Transport Model (CTM) CHIMERE-DUST was used to simulate the mineral dust cycle over the Sahara in 2006 [Schmechtig et al., 2011]. In this case, the model is forced by meteorological fields supplied by the European Center from Medium-range Weather Forecasts (ECMWF). To test the capability of the model to reproduce the dust load and surface concentrations from daily to seasonal time-scale the ground measurements from African Monsoon Multidisciplinary Analysis (AMMA) field campaign were used. The ability of the model to describe the altitude of the dust transport was tested for the cases of low and high altitudes. Vertically, 15 levels are defined from the surface to 12 km (200hPa), the first layer

of the model extending from 0 to 54m.

The ground based stations collected measurements of atmospheric concentrations of particulate matter smaller than 10μm by collection of samples and the corresponding later analysis of them. This process was carried out with the help of purpose built wind oriented inlets. Regarding the analysis of the description of the surface concentration not high values were expected from the beginning because the domain of the model for this parameter was 54m height considering a well mixed layer while the measurements were done from the surface to 6m-9m height where the inlet of the measurement instrument was placed.

On the other hand, in the comparison of model with LIDAR results, authors mentioned that the vertical profiles of backscatter signal due to the presence of mineral dust obtained by means of the LIDAR measurements of a dust event made in Niamey-Niger [Slingo et al., 2008] were correctly simulated by the model.

In spite of the qualified as well reproduced episodes, authors conclude that there is a need of further exploration on the vertical distribution, the dust size distribution and the deposition fluxes.

CHIMERE-DUST case study II: Comparison of mineral dust layers vertical structures modelled with CHIMERE-DUST and observed with CALIOP LIDAR

Here the authors evaluate the capability of CHIMERE-DUST model to simulate the mineral dust vertical distribution and transport by using profiles coming from CALIOP LIDAR [Vuolo et al., 2009]. They analysed about 170 000 vertical profiles of light backscattered by aerosols within a six months period. Here the meteorological fields from the Global Forecasting System (GFS) of NCEP are used to force the MM5 model. As starting point they excluded the clouds and no mineral aerosol layers. They found that regarding dust occurrence the model observations agreement within the same profile is between 60 and 80%. In general the model behaves quite well far from the emission regions, but errors on the thickness of the mineral dust

layers can be from 50% in summer and 100% in winter, while the maximum value of the LIDAR signal can be underestimated by 30%. They say that due to computer limitations the model can't reproduce the fine physics of multi-layered structures like those of the free troposphere that is made up by thin consecutive sub layers. Thus, it offers data with vertically averaged layers. As a result, thin dust layer long range transport is not well represented, so producing overspread profiles compared to observations with CALIOP. Authors suggest that the models vertical mixing is excessive and they conclude that the model is not able to run over a large space and time range.

To estimate the dust occurrence authors define two values: 1 when incidence of dust and 0 when no dust. Under this definition they apply the sum for all the values of each of the 30 vertical layers during one season. After the suitable average of LIDAR data to adjust the grid to the model's resolution, the comparable results were generated and they are presented in the figure 3.17.

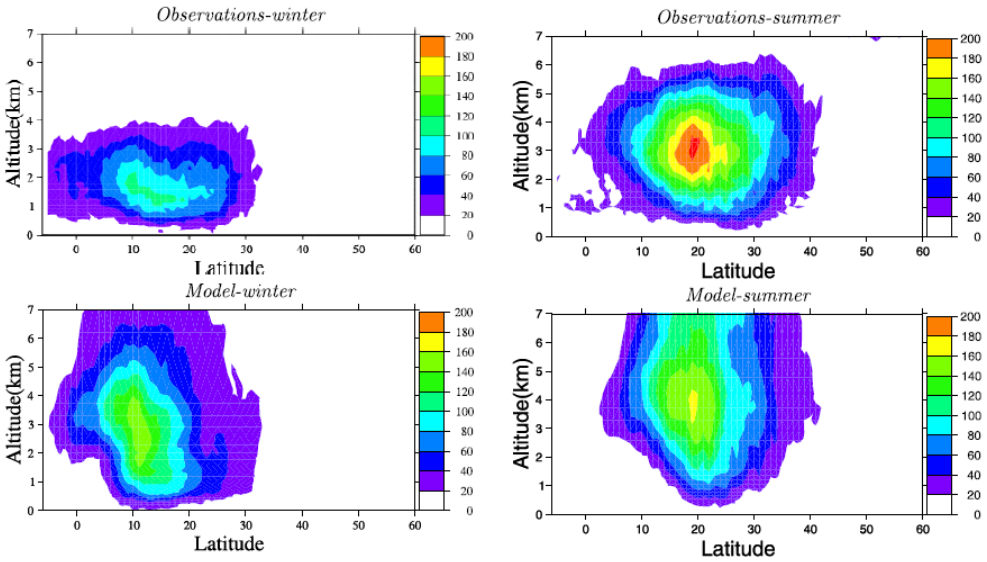

Figure 3.17: Comparisons of the results CHIMERE-DUST and from CALIPSO observations of the seasonal dust occurrence (winter, left and summer, rigth) along the showed latitude stripe in the geographical model domain. [Vuolo et al., 2009].

3.4.3 DREAM

Dust REgional Atmosphere Model (DREAM) is a regional model designed to predict the atmospheric cycle of mineral dust. The model has cells defined as deserts where surface dust injection is considered. In these zones some dust injection is assumed in the properly parametrizated production phase. Once the injection of dust has taken place the aerosol is driven by diverse atmospheric variables and processes like turbulence in the first stage, then winds and finally thermodynamic and deposition processes [Pérez et al., 2006b].

DREAM case study I: A long Saharan dust event over the Western Mediterranean: LIDAR, Sun photometer observations, and regional dust modelling

In this study [Pérez et al., 2006a] backscatter LIDAR observations and sun photometer data of a long event of Saharan dust transport toward the western Mediterranean from some stations of EARLINET and AERONET respectively serve the evaluation of the dust model DREAM. The authors point out that the LIDAR installed in the Barcelona station provides useful signal from 300m up to 1 500m a.s.l. The figuire 3.18 illustrates some comparisons of modelled predictions with observational data retrieved in 2002.

Authors consider that the daily evolution of dust vertical structure observed by the LIDAR over Barcelona is well captured by the model.

In the regions of Avignon and Arenosillo it was identified the mixture of mineral dust and anthropogenic aerosols in the boundary layer by means of the sun photometers measurements. Authors clarify that the scope of the study is not to evaluate surface concentration which should be performed against regional background air quality stations with weak influence of anthropogenic pollution.

Finally they consider that the modelled vertical profile which 24 layers extend up to 15km is in a good agreement with observations although they have a tendency towards overpredicition in the upper levers of a dust plume.

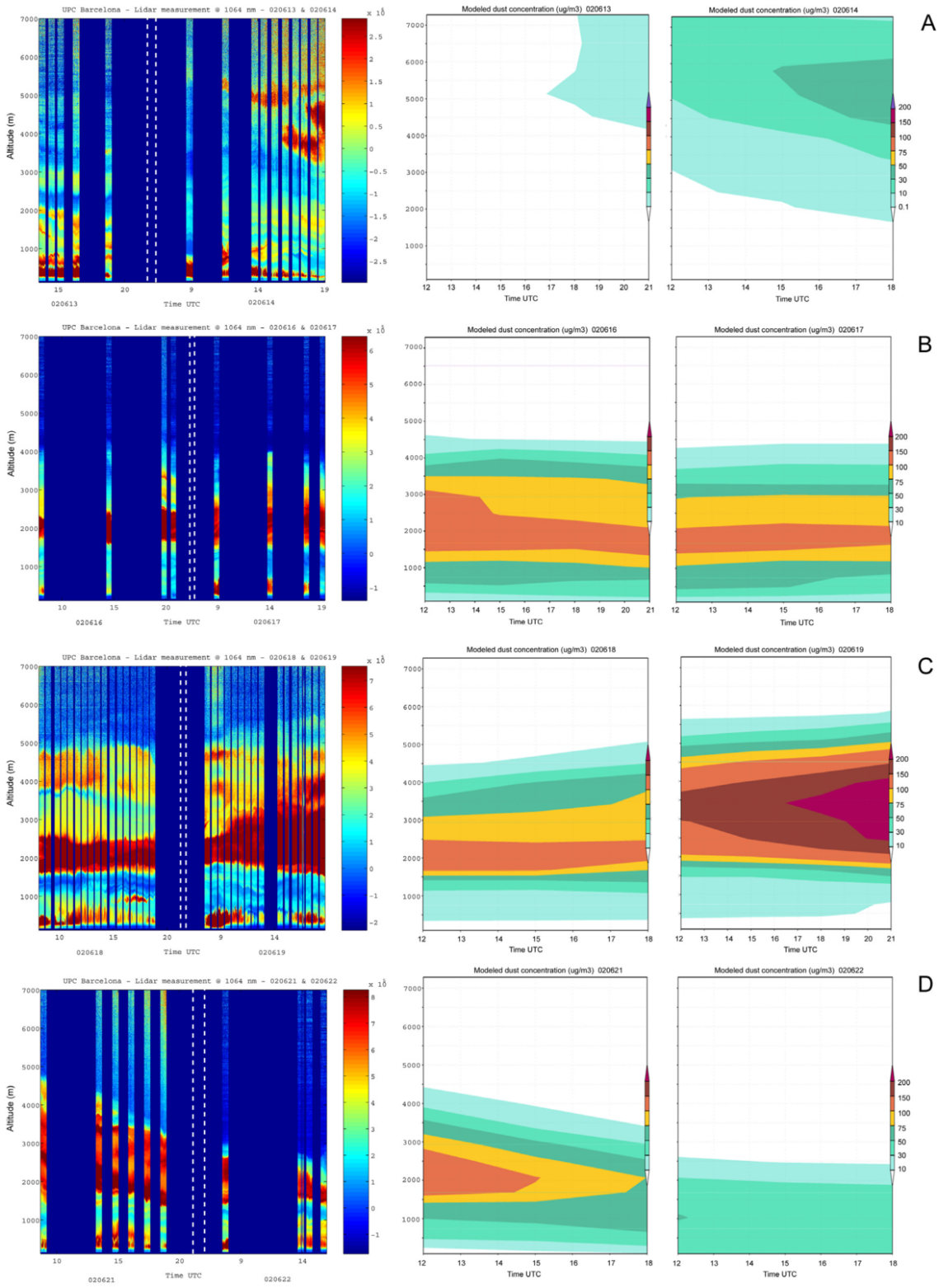

Figure 3.18: 1064nm corrected LIDAR signal and the corresponding modelled vertical dust concentration over Barcelona on A: 13^{th}-14^{th} June. B: 16^{th}-17^{th} June. C: 18^{th}-19^{th} June. D: 21^{st}-22^{nd} June. [Pérez et al., 2006a].

In brief, respect to the suitability of different devices to characterize aerosols in the lowest part of the troposphere, it is possible to say that instruments for making ground-based measurements mostly (except LIDAR) are not able to profile vertical structures. For its part although LIDAR can profile vertical distributions, it has a problem of reliability of data in the near-ground zone due to the overlap function. To solve the problem, remote sensing techniques assisted by nadir-viewing LIDARs aboard aircrafts or satellites are applied. The only way valid until the moment to profile vertical structures with measurements from space has been using active instruments since passive techniques like imagery deliver total values that represent the effect of cumulative contributions up to the TOA. Compared to LIDAR ground-stations, satellite LIDAR instruments (CALIOP) provides wider coverage and uniformity of data but due to the orbital periods of the satellite it is not the most appropriate tool to follow reliably events of quick temporal evolution. For that purpose LIDAR ground-based networks by applying the required corrections could approximate in a better way the representation of those events. On the other hand, models are an alternative approach that has its limitations in some factors like the high computational capacity required, the need of time for processing of data, the need of precision in models that allow reproducing as faithfully as possible the complex atmospheric processes and the interrelation among them in the PBL. However the flexibility of modeling techniques to generate the desired output under certain conditions makes the models an option that still can be improved.

Most of the studied cases had as common approach the big scale analysis of aerosols in the atmosphere and the analysis of the near-ground layer was out of the proposed scope. Because of this and the lack of coincidence in the geographical area under research,it is not expected to have a reference point to compare the results of this study.

CHAPTER 4

Treatment of Satellite Data

Given the advantages of satellite data and the condition of CALIPSO of being a relatively unexplored tool to extract information in the near-surface looking towards solar applications, data provided by CALIOP module has been retrieved and processed as will be described in the next sections.

4.1 CALIPSO underlying retrieval algorithms and data

To provide some background information about the satellite, through this section a summarized review of the most relevant assumptions, procedures, definitions and terminology associated to CALIPSO's retrieval of data from its scientific and technique conception are presented.

To start, it is worth mentioning the basic terminology employed by CALIPSO literature, which is as well used in this document.

Feature is the term that describes any extended and continuous region of enhanced backscatter signal that rises significantly above the expected molecular value;

encompassing clouds, aerosol and surface, and excluding in turn noise occurrences. Formally the 8 types of features reported by CALIPSO [NASA, 2011] are:

1. Invalid (bad or missing data)
2. Clear air (this does not mean pristine air but it indicates the cases where although the signal was not totally attenuated there was not identified feature)
3. Cloud
4. Aerosol
5. Stratospheric cloud or stratospheric aerosol
6. Surface
7. Subsurface
8. No signal (totally attenuated)

But how CALIPSO determines the listed features? First CALIPSO establishes which is the spatial extension of the feature and then it identifies which of the possible object or feature (listed above) is it. It does it within each profile (total vertical column measured in a certain pair latitude-longitude).

The feature identification process is accomplished by means of an algorithm called CAD (Cloud Aerosol Discrimination) that provides as well a confidence level on the classification. The discrimination between aerosols and clouds is accomplished by a so called confidence function based on the PDFs (Probability Distribution Function) of both features. This functions have as input the following measurable attributes of each feature. For the case of products version 3 these attributes are the mid-feature altitude, the feature mean attenuated backscatter at 532nm, the feature integrated attenuated total color ratio, the volume depolarization ratio and the latitude.[Liu et al., 2010].

Once this identification has been done, a new process aims to determine aerosol and cloud subtypes among others through the additional Scene Classification Algorithms (SCA). After those stages, the retrieval of optical properties is done. The possible responses in the CALIPSO subtype analysis in the case of aerosols are:

1. Not determined
2. Clean marine
3. Dust
4. Polluted continental
5. Clean continental
6. Polluted dust
7. Smoke
8. Other

Similarly, the cloud subtype classification can bring the following results:

1. Low overcast, transparent
2. Low overcast, opaque
3. Transition stratocumulus
4. Low, broken cumulus
5. Altocumulus
6. Altostratus
7. Cirrus
8. Deep convective, opaque

CAD algorithm was developed by the CALIPSO team in the beginning with help of the evaluation of computational model predictions of two properties of the particles: the intrinsic (depending only on the type of particle, independent of the concentration of particles in a unit of volume) and extrinsic scattering (depends on the particulate amount in the volume). In the next step of the preparation of this algorithm, from both scenarios the possible values of the backscatter color ratio $\chi = \beta_{1064}/\beta_{532}$ of the several feature types were analysed. It intended to identify a pattern by type of particle according to the shape by means of χ. Since the size of cloud particles is quite large with respect to the wavelengths used by CALIPSO instruments, the expected variation of the backscatter coefficient in both cases (1064nm and 532nm) is so low that the foreseen color ratio is roughly 1. On the contrary, most of aerosol' sizes are smaller so that they can be affected by the laser beam and they exhibit different responses to the two LIDAR wavelengths in a way that a pattern can be identified.

4.2 Use of CALIPSO data in this study

As mentioned in the objectives section this study aims to present an estimation of the one-year averaged AOD for the columns of air from ground to 120m - 180m[a], and to 8,2km and the corresponding ratio between them in order to observe the contribution of the lowest part respect to the larger section. The latter can be considered as total since it could be said that this height usually contents nearly the totality of aerosol particles. The oscillation of values of altitude in the lowest range (120m to 180m) is due to the shift of the height covered because the effect of vertical resolution on the variations of relief.

Since the focus of this study were aerosol particles and they are involved in scattering as much as in absorption processes, the available variable in the Scientific Datasets of CALIPSO that could depict both influences (refer to the definition in

[a]Asociated with the averaged vertical resolution of datasets/VFM flags and because of the reference level of CALIPSO is the mean sea level and the information is provided from -0,5km, the presence of reliefs can entail a variation of the actual height of the measurements.

the chapter 2 in page 9) was the Extinction Coefficient κ. For the analysis there was no discrimination of aerosol by subtype, all of them were taken into account.

4.2.1 Choosing products

Given the requirement of having data per altitude segment (not totally attenuated products) of the variable of interest (Extinction Coefficient 532nm), the available CALIPSO product that fits in such necessity belongs to level II set of products. To have a context about the formats in which typically data products of Earth Observation Systems (EOS) are processed the standard levels are briefly described as follows[b]

Level 0 unprocessed instrument and payload data at full resolution removing synchronization frameworks, headers and duplicated data.

Level 1A unprocessed instrument data at full resolution, time-referenced with appended information like georeferencing parameters.

Level 1B (not always present): data have been processed to be presented at sensor units.

Level 2 derived geophysical variables from data at level 1 at the same resolution of that level.

Level 3 Variables have been processed to be mapped on uniform space-time grid scale. They have usually with some completeness and consistency.

Level 4 Results from analyses of lower-level data, like variables obtained by processing of multiple measurements.

The three standard format of CALIPSO level II data products used in this study are:

1. VFM (Vertical Feature Mask).

[b] `http://science.nasa.gov/earth-science/earth-science-data/data-processing-levels-for-eosdis`

2. Cloud and aerosol layer products.

3. Cloud and aerosol profile products.

From those in this study the VFM and the aerosol profile products were used (1 and 3). It is important to note that although there is a linkage between VFM and the aerosol profile product they are available in two separate files with different horizontal and vertical resolutions.

The VFM data consist in an array of integers that characterize the spatial distribution of clouds and aerosols in different vertical and horizontal resolutions by describing the presence of certain feature and its corresponding subtype as it applies to. The arrangement of flags is illustrated in figure 4.2. This product was used because of the following reasons:

1. The required optical information must come only and exclusively from aerosols and since the presence of most clouds could represent an interference factor for the reliability of the read-outs, the profiles that contain such type of clouds must be removed from the database to be analyzed.

2. Likewise the flags provided by the VFM helped to locate the surface (considering the ground level variations) and from there to verify the existence of optical information (from the profile product) in the altitudes of interest. Thus, the flags of the VFM provided the information to select the valid profiles to be analyzed.

3. The selection of valid profiles also took into account the presence of dense or opaque clouds, dismissing all those columns containing clouds different than cirrus, because they are thin and virtually transparent enough to be considered as components with low interference in the measuring process of lowest features by LIDAR. The total absence of clouds was not considered as criteria because it would have restricted even more the amount of available data to be processed.

The profile products provide information about the optical properties with ancillary descriptors of the temporal and geophysical conditions for each one and a

meteorological context that includes among others temperature, and atmospheric pressure. The optical properties are supplied by means of mapping the vertical distribution of extinction and backscatter coefficients for aerosols.

In order to estimate the quality of the data retrieved from CALIPSO, comparisons with data coming from independent sources have been made by the CALIPSO developers team. The measurement of the level of accordance of CALIPSO data with regard to proven models is called maturity. In this study the highest maturity available for each product has been used. Since every parameter exhibits different uncertainties CALIPSO data is classified as well in different categories. The maturities and uncertainties are defined as follows:

Beta Early released data recommended to the do the first approaches to become familiar with CALIPSO data. No comparisons with other sources are made.

Provisional Some limited comparisons with independent data have been made. Some obvious artifacts defined as false effects and results that are not manifestations of the measured phenomena but owing to the experimental arrangement are as well fixed in this level of data treatment.

Validated stage I Comparisons are based on measurements made on selected locations and times.

Validated stage II Similar to validated stage but with a larger number of measurements more widely distributed.

Validated stage III The comparisons are made with global measurements.

Versions used

As a result, from the different products and versions those that were chosen as source of information for the present study are:

- PRODUCT 1
  - Type of product: LIDAR aerosol level 2 scientific data set

  - Name of the product: Aerosol Profile Data Product DP 2.1B
  - Major version: V3
  - Minor version: 01
  - Maturity level: Provisional

- PRODUCT 2

  - Type of product: LIDAR level 2 Vertical Feature Mask
  - Name of the product: Vertical Feature Mask Data Product DP 2.1B
  - Major version: V3
  - Minor version: 01
  - Maturity level: validated stage I

The mentioned scientific data set contains the optical variable that was processed with the aim of obtaining the aerosol optical depth AOD (Extinction Coefficient) in the altitude range of interest. The indicated choice was done as well because the mentioned versions have the improved version of feature classification algorithms, they have the largest amount of available data and they have in its corresponding type of product the highest available maturity level.

4.2.2 Selection of spatial ranges

Geographical Region

As indicated in the objectives section, the considered region for this analysis covers the area contained between longitudes 15°W and 40°E and the latitudes 20°N and 45°N. (Figure 4.1). At data processing, one degree was the cell size that offered the best trade off between density of points and resolution. The final maps were generated using this resolution.

Figure 4.1: Geographical area of coverage for the study.

Vertical and Horizontal Ranges

The choice of the vertical range of interest considered two important aspects:

1. The directly relevant altitudes for the CSP solar plants depend on the height of the tower, of which the measure ranges around 100m and 200m above the ground.

2. Then, considering the predominance of desert conditions in the target region, dust transport becomes an important factor to take into account. Dust loads could have a high occurrence in some areas of interest and they play an important role in the extinction of solar radiation. As the dust moves away from its origin, it spreads and is lifted as high as 7km (documented in central Europe) [Bösenberg and Matthias, 2003].

Taken into consideration the aforementioned factors and to take advantage of the uniformity of the flags structure in the first 8.2km, the latter was chosen as the maximum value of altitude for the analysis of data. The considered altitude can be distinguished in the blue-shaded box of figure 4.2, which also shows the gridded structure of the flags provided in the VFM files.

The flags data structure has different vertical and horizontal resolution compared to the SDS that contains the optical properties. Whereas the horizontal resolution

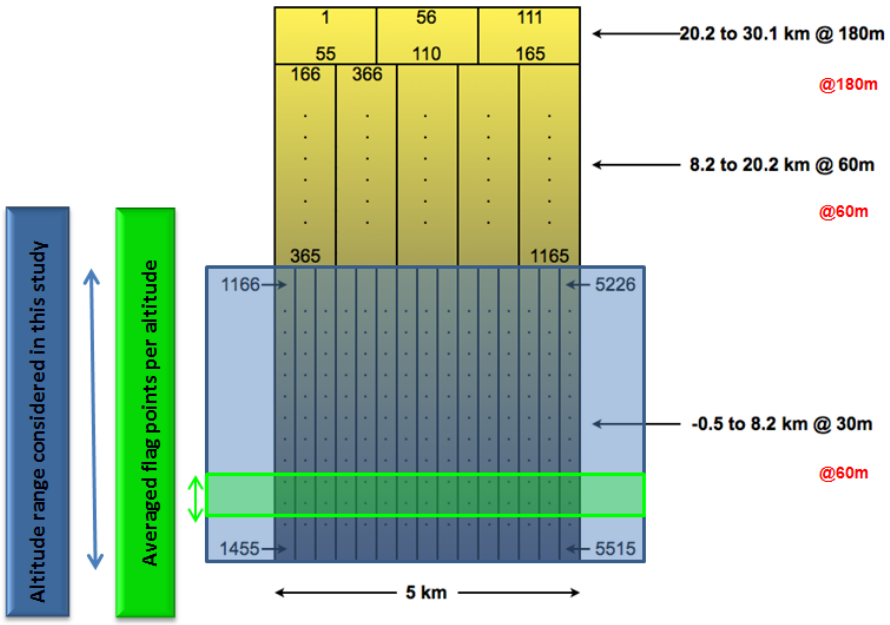

Figure 4.2: Structure of flags provided in the VFM files of CALIPSO data. The blue-shaded area represents the vertical section considered in this study. The green shaded stripe indicates that in order to standardize the resolutions it was necessary to process two rows of 15 profiles 333m wide each one to obtain an equivalent corresponding to one value of Extinction Coefficient (one altitude). The values in black (right) correspond to the resolutions per each indicated vertical segment in the VFM files. The red values indicate the corresponding values for the SDS of aerosol profiles.

of the profiles containing the Extinction Coefficient is 5km, the corresponding value for the flags structure varies from 333m (15 profiles in 5km) in the lowest range of altitude, through 1km in the medium heights, up to 1.6km in the top part of the sensed atmosphere. The horizontal range of the data processed for this study was limited by the one with less horizontal resolution, what means 5km. Similarly, although both profiles (optical properties and flags) have segmentation on resolution in the vertical domain, the flags array has double resolution in the lowest segment, what means that per each altitude in the Extinction Coefficient profile there are two rows of data provided by the flags. The indicated differences in horizontal and vertical resolutions implied the need of a strategy that allowed determining the dominant feature per each valid altitude of the Extinction Coefficient profile from flags array. It was done by mean of finding the highest occurrence (also known as the mode) of each feature among the 30 points per altitude (see the green stripe in figure 4.2). For the obtained maps the vertical resolution remains unchanged.

4.2.3 Retrieving optical properties

With the aim of depicting to what extent aerosol presence reduces the incoming irradiation in the first 150m above ground, AOD derived from the Extinction Coefficient was the optical parameter considered as the final variable of interest. As described in the section Theoretical Basis AOD is formally defined as the integral of the extinction coefficient with respect to distance. For this particular case it can be also expressed as the sum of all discrete contributions per altitudes, as shown in the equation 4.1.

$$AOD_{Layer} = \sum_{0}^{Subscript_{TOL}} \kappa * 0.06km \tag{4.1}$$

AOD_{Layer} : Aerosol Optical Depth of the considered layer

$Subscript_{TOL}$: Subscript of Top Of Layer

κ : Extinction Coefficient

Where AOD_{Layer} is the aerosol optical depth of the considered layer, in this case it can be either 150m or 8.2km. The low limit of the sum is 0 that is the first valid measurement at the altitude (corresponding to the zero level above ground). $Subscript_{TOL}$ means Subscript of Top Of Layer that denotes the subscript of the discrete segment of altitude that is considered. The Extinction Coefficient κ is multiplied by 0.06km since the vertical resolution of the optical variables is 60m. It is important to notice that the vertical profile is created only when there are valid values of κ in the layer of 150m and when the cloudiness condition is met as explained in the section 4.2.1.

CHAPTER 5

Results

The satellite data was processed as described in chapter 4. As result, a set of maps were generated and they are listed as follows:

AOD 150m The AOD for an air volume (per cell of the grid) of 1° wide, 1° long and 150m height referred to ground level.

Total AOD The AOD for an air volume (per cell of the grid) of 1° wide, 1° long and 8 200m height referred to ground level.

Ratio A percentage that describes the contribution of *AOD 150m* to *Total AOD*.

Density of data points for each grid cell for the specified year and day cycle. It means it reflects the number of measurements in each cell with dimensions of 1° x 1° along 8 200m height.

Those illustrations were produced for 2007 and 2008 for both day and night profiles for a total of 16 maps. In addition one histogram was generated per dataset. There it is possible to observe the distribution of values of each map.

By using the histograms, the appropriate scale range for each map was determined. Thereby the maximum among all the values collected does not define the scale for the graphs. Instead of that the limit of the scale is that one that contains the most significant amount of data. The intention is not to present the peaks of each variable, but rather to maximize the presentation range in order to discriminate better between the data values. The referred histograms are presented here in figures: 5.1, 5.2, 5.3, and 5.4.

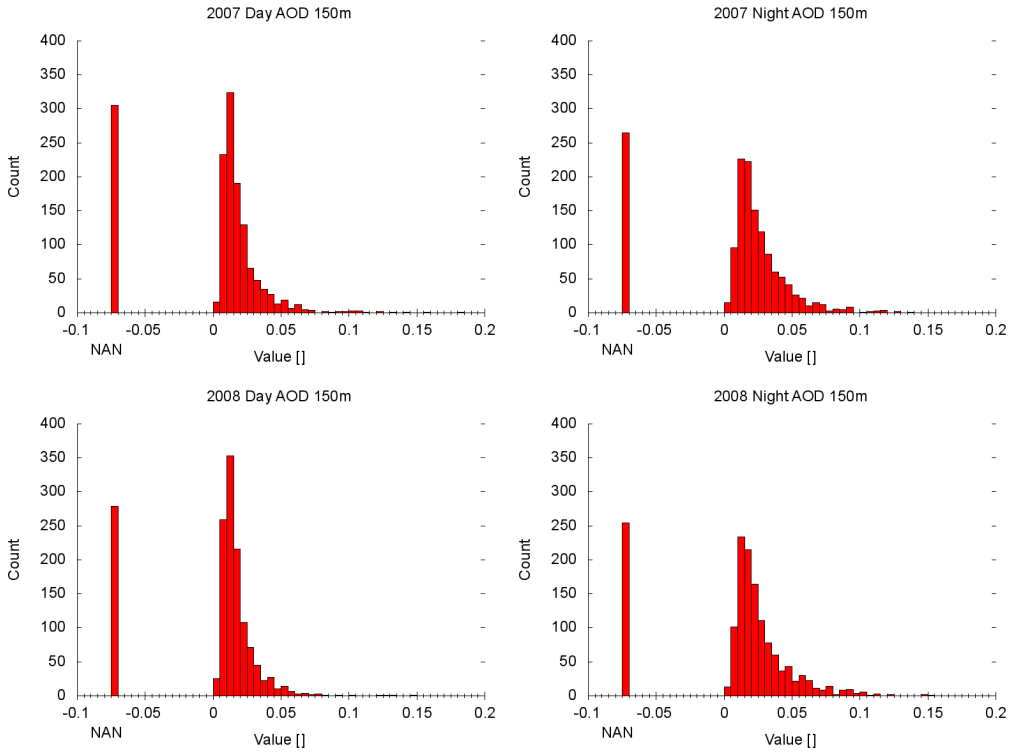

Figure 5.1: Histograms of the AOD calculated for a height of 150m.

The Not a Number (NAN) values represent for every case the number of cells among the total of 1 375 that do not have any valid value.

The final scales are summarized in the table 5.1.

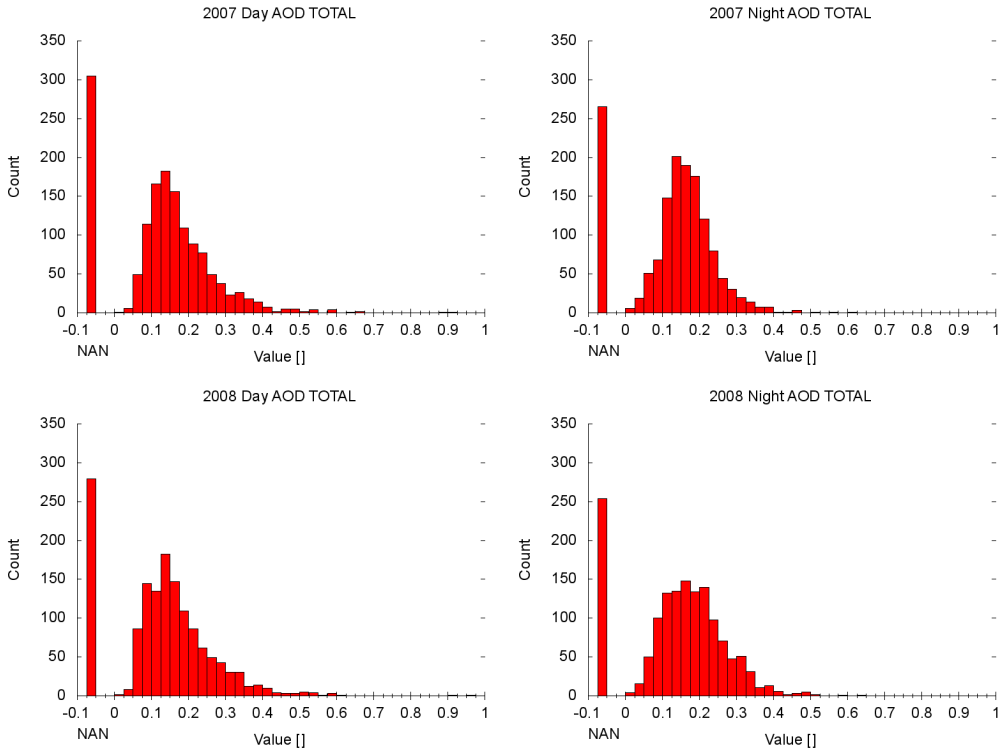

Figure 5.2: Histograms of the Total AOD calculated for a height of 8.2km.

Map type	**Minimum scale value**	**Maximum scale value**	**Units**
AOD 0 - 150m height	0	0.125	[ ]
AOD 0 - 8.2km height	0	0.4	[ ]
Contribution of AOD 150m to total	0	35	[%]
Density points	0	400	[samples]

Table 5.1: Depending on the histograms, the ranges for the different maps have been selected.

5.1 Relative Errors

The data is supplied by CALIPSO with the absolute errors of each measurement of the extinction coefficient κ. The table 5.2 summarizes the distribution of the calculated relative errors on the samples handled.

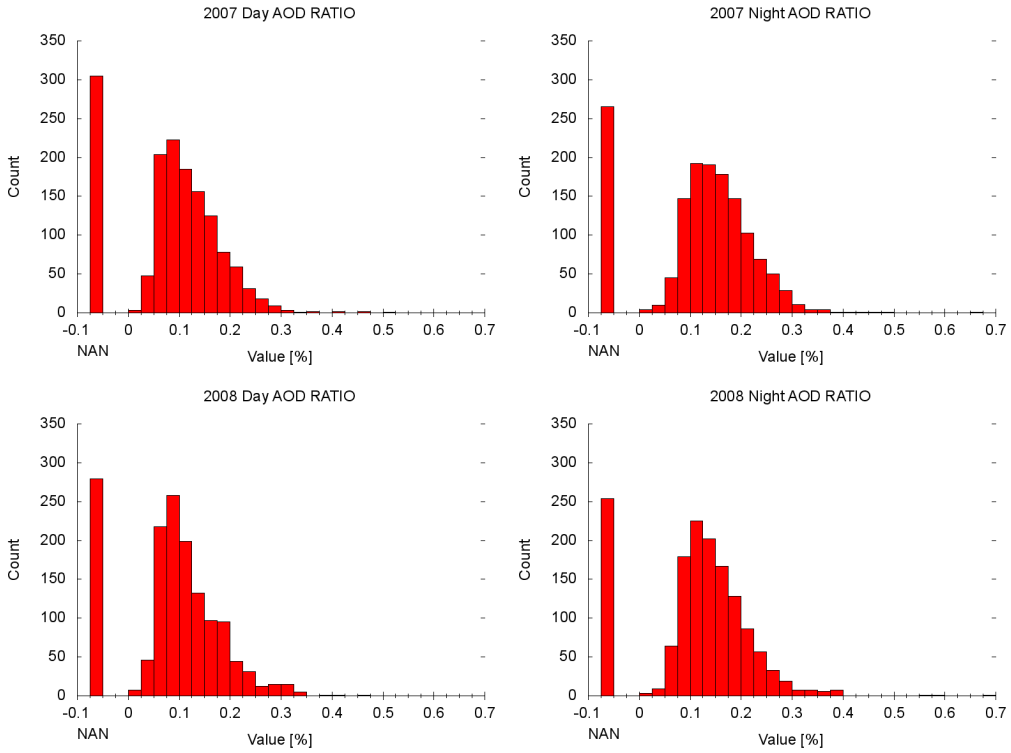

Figure 5.3: Histograms of AOD contribution ratio 150m over total.

Relative Error Interval	**Percentage of samples**
$< 30\%$	0.06%
$[30\%, 50\%]$	1.95%
$[50\%, 70\%]$	10.70%
$> 70\%$	87.28%

Table 5.2: Distribution of the relative error in κ as supplied by CALIPSO

Despite of being high, the error amounts are well aligned with the typical values found in some remote sensing devices.

One important remark is that no error propagation has been calculated for the maps given as result. But the table 5.2 gives a rough idea of the expected uncertainty levels in the final determination of the AOD.

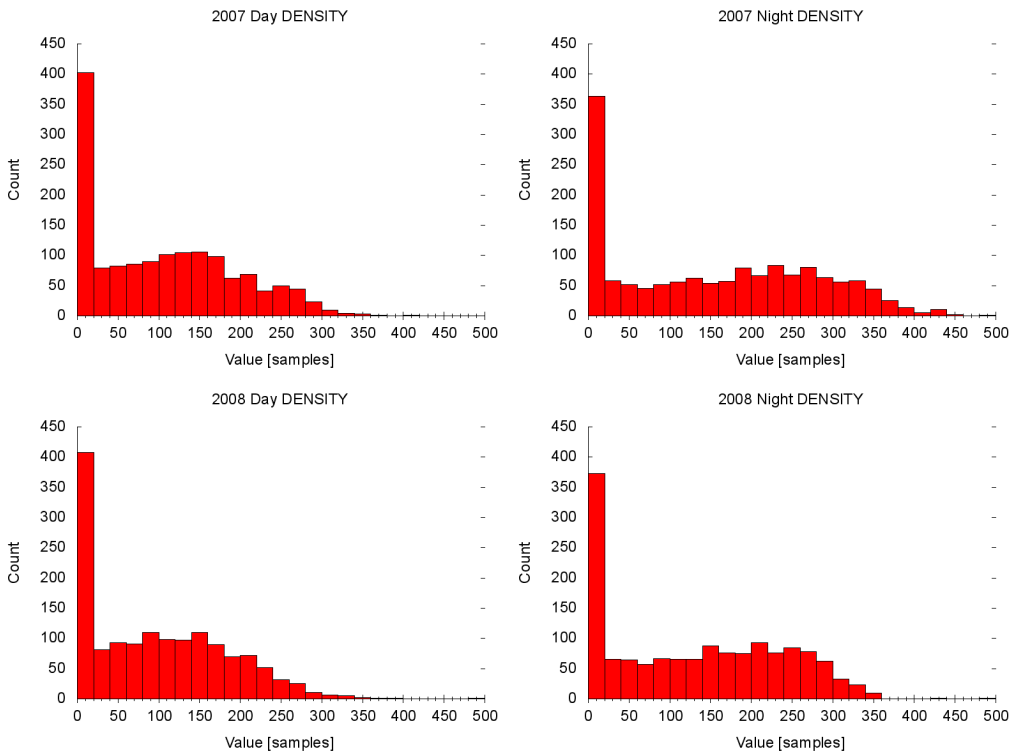

Figure 5.4: Histograms of the AOD data density.

5.2 Output maps

In general for both years a pattern on certain zones with more presence of aerosols can be distinguished.

Regarding the AOD observed in the lower layer of 150m, except for some points, the patterns in daytime profiles in 2007 and 2008 looks very similar. For both years the highest values can be observed in Morocco, the Iberian Peninsula, North and South Algeria, Middle Libya, Northeast Egypt, Israel, West Syria, Turkey, the West coast of Saudi Arabia at the Red sea from South Sinai to the height of the Nubian Desert. Likewise the night-time profiles of both years do not differ significantly between them. However it is possible to notice disparities between day and night on each year. The night-time values are enhanced and can be up to five folded respect to those of daytime. This rise of values can be observed especially in the highlighted above mentioned places as well as Tunisia.

About the ratio between the AOD in the first 150m respect to the value along

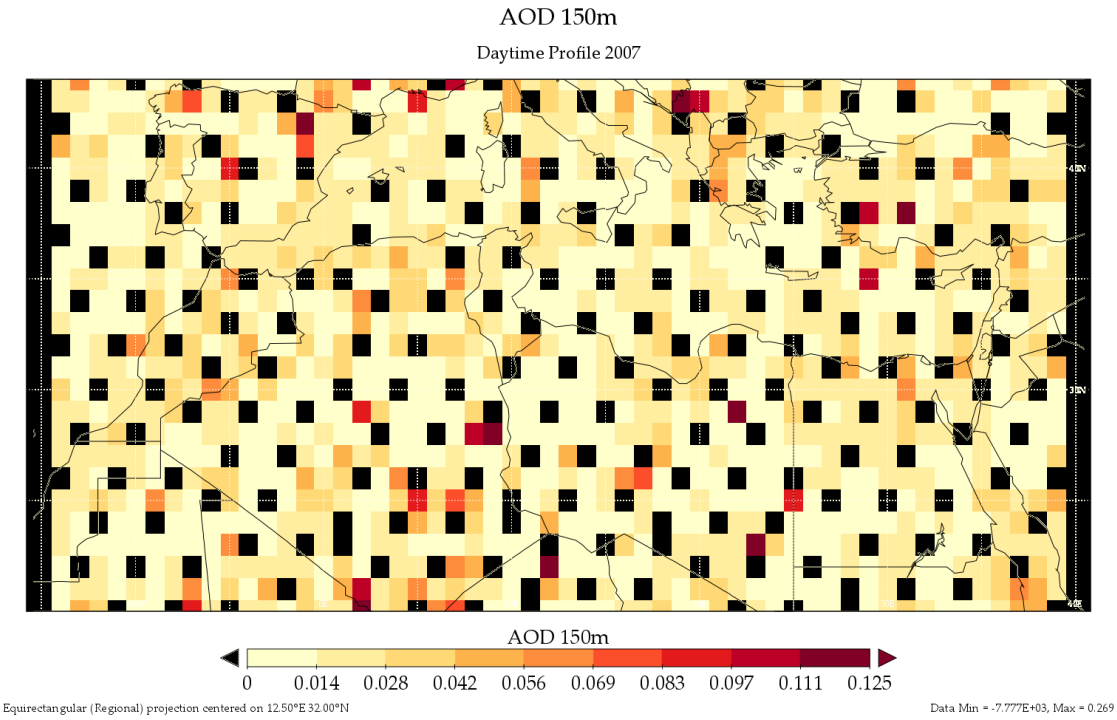

Figure 5.5

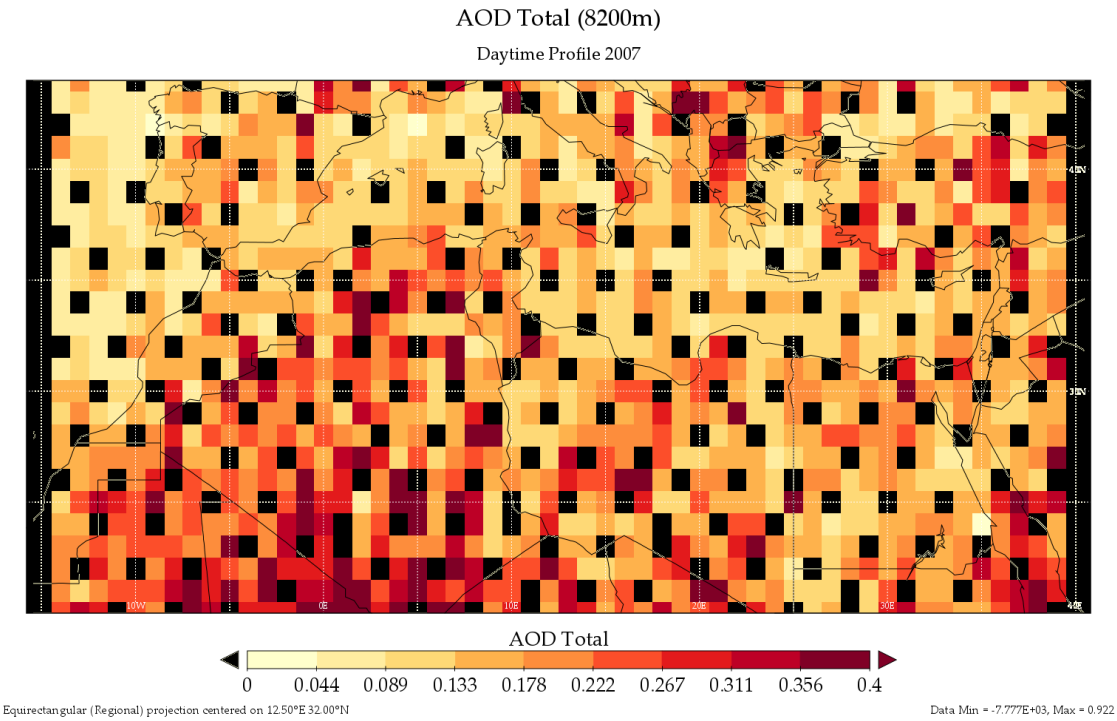

Figure 5.6

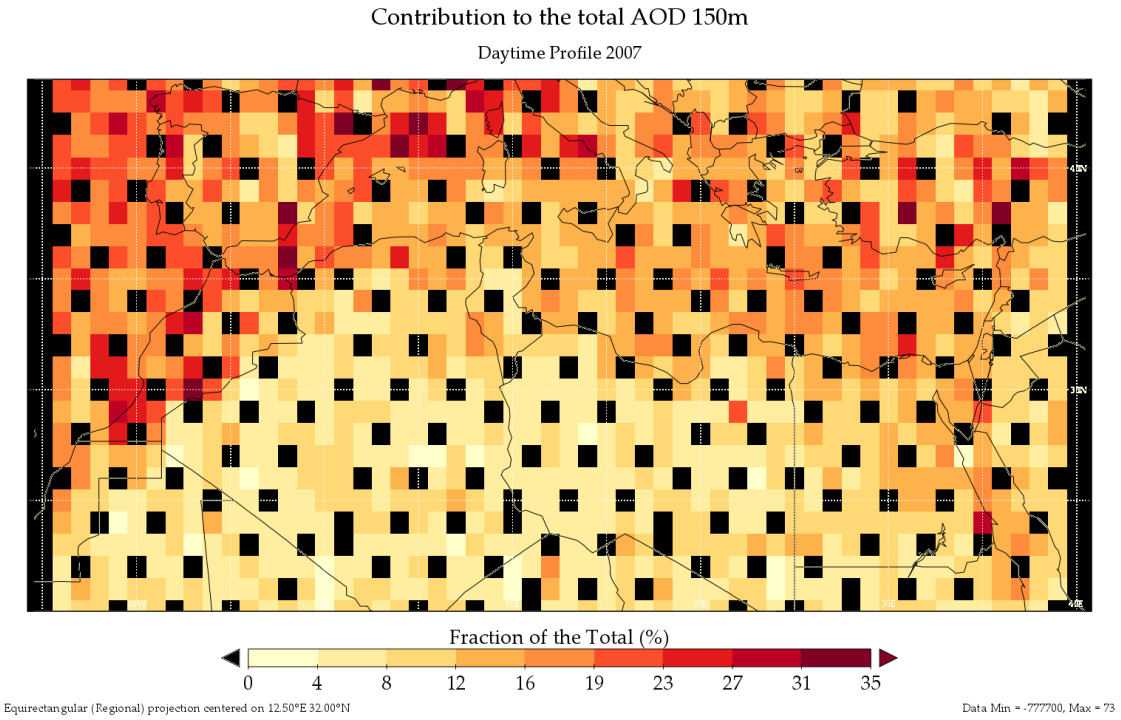

Figure 5.7

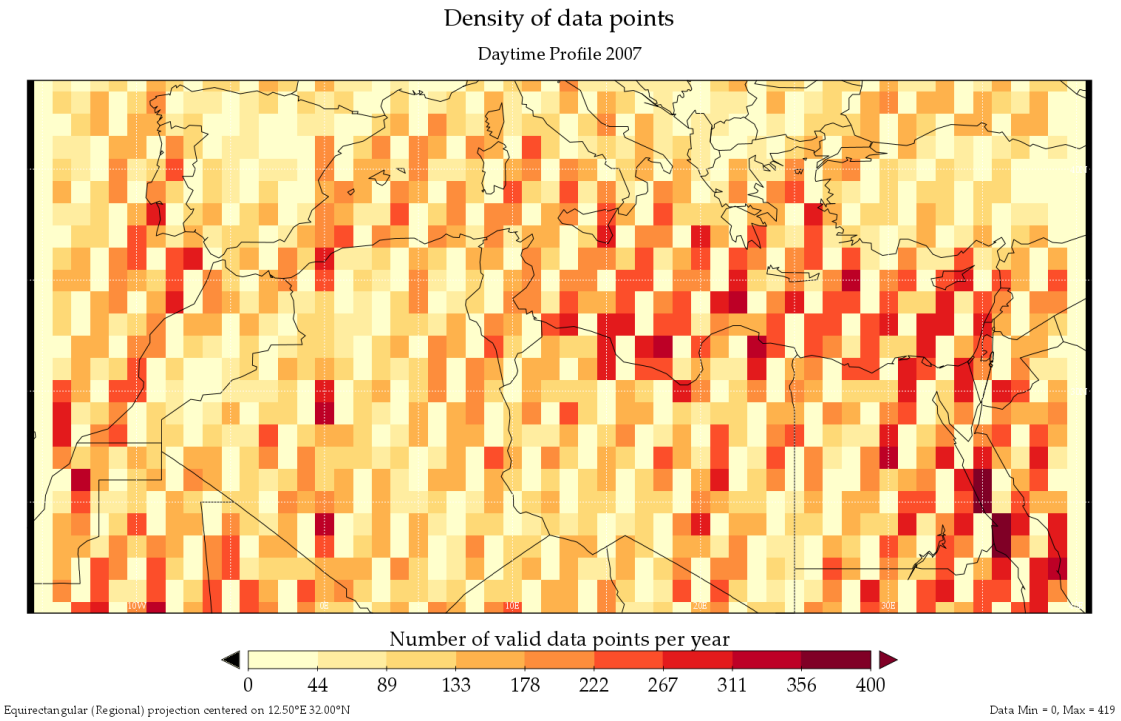

Figure 5.8

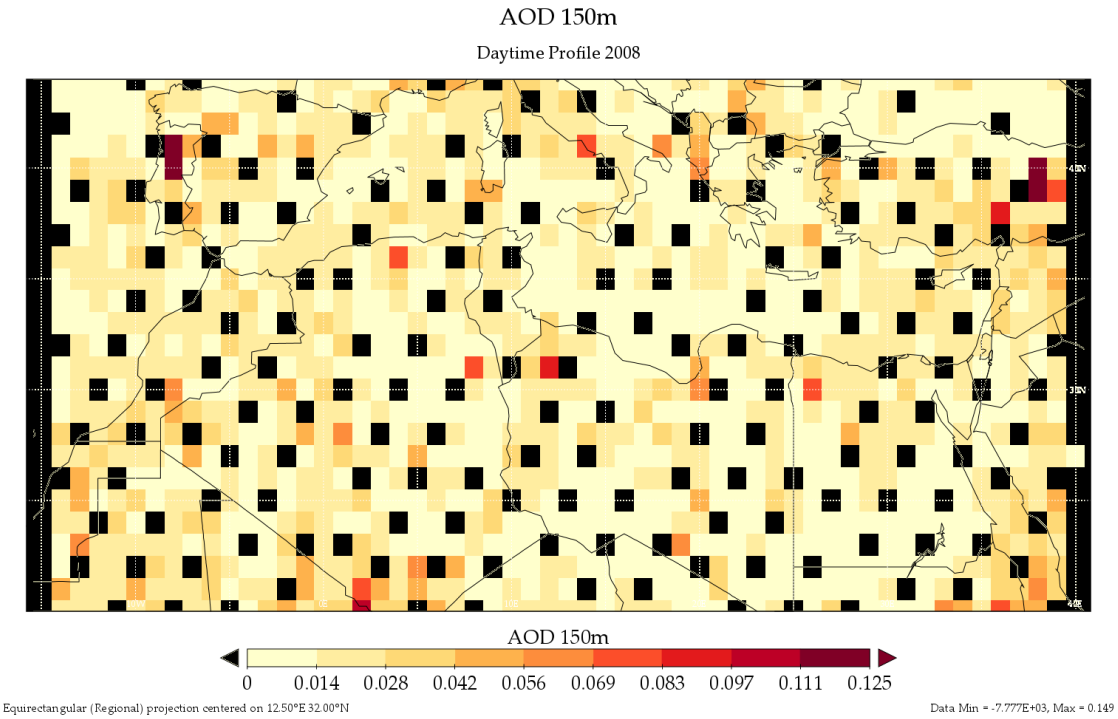

Figure 5.9

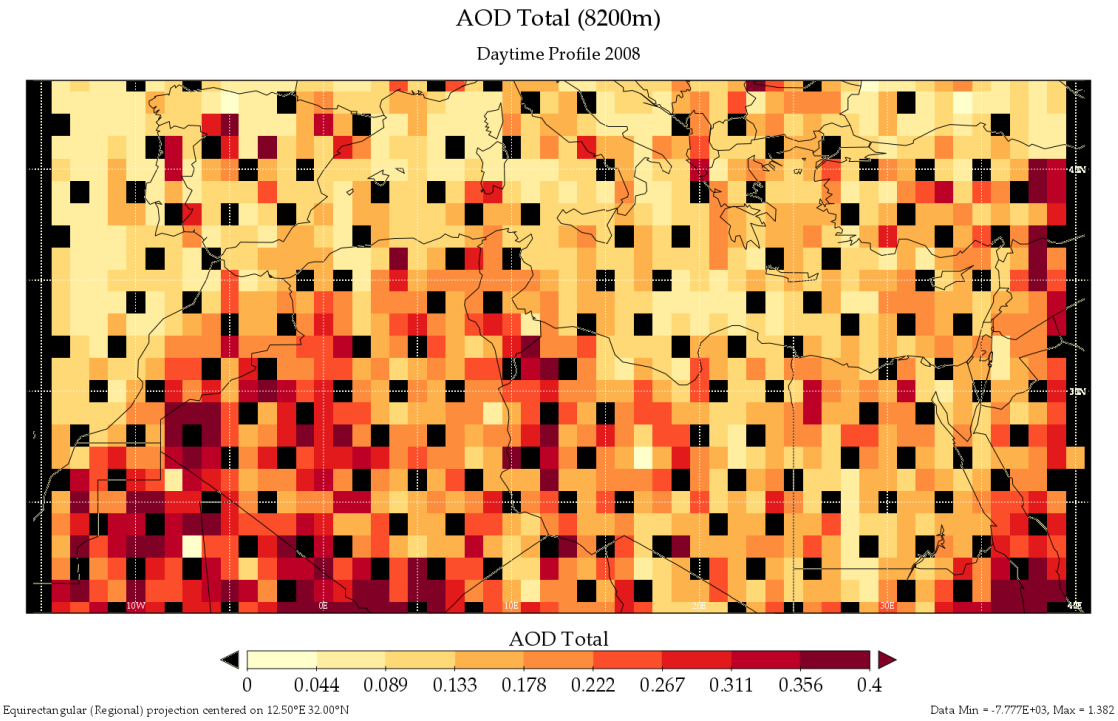

Figure 5.10

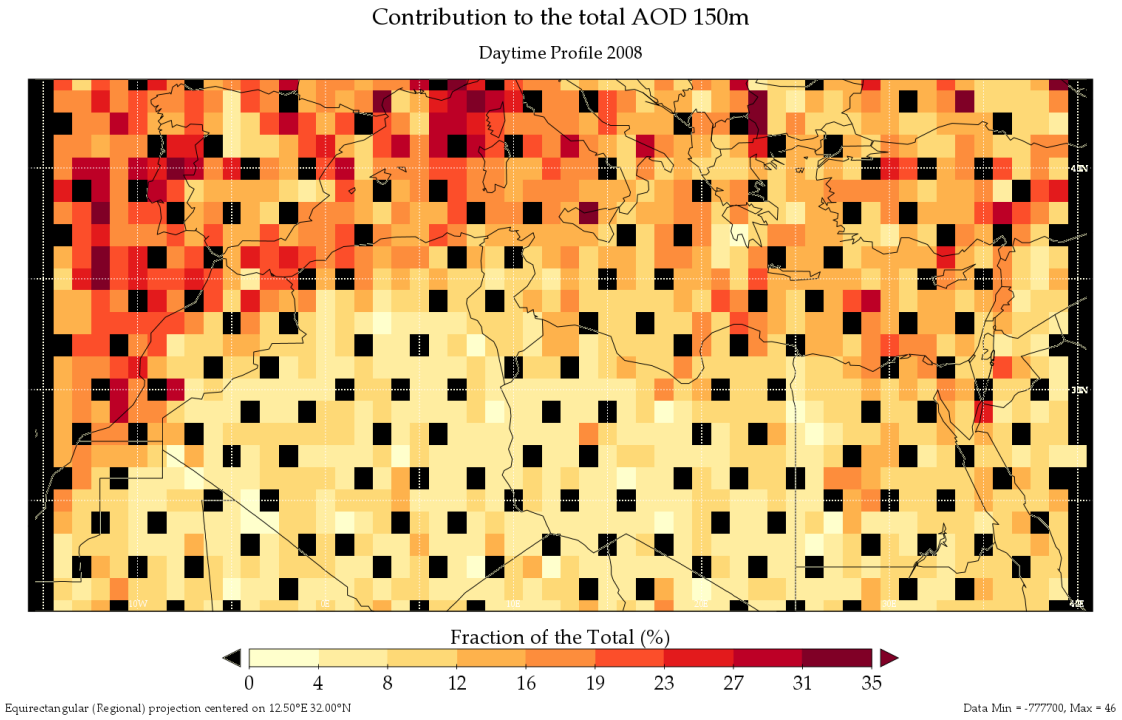

Figure 5.11

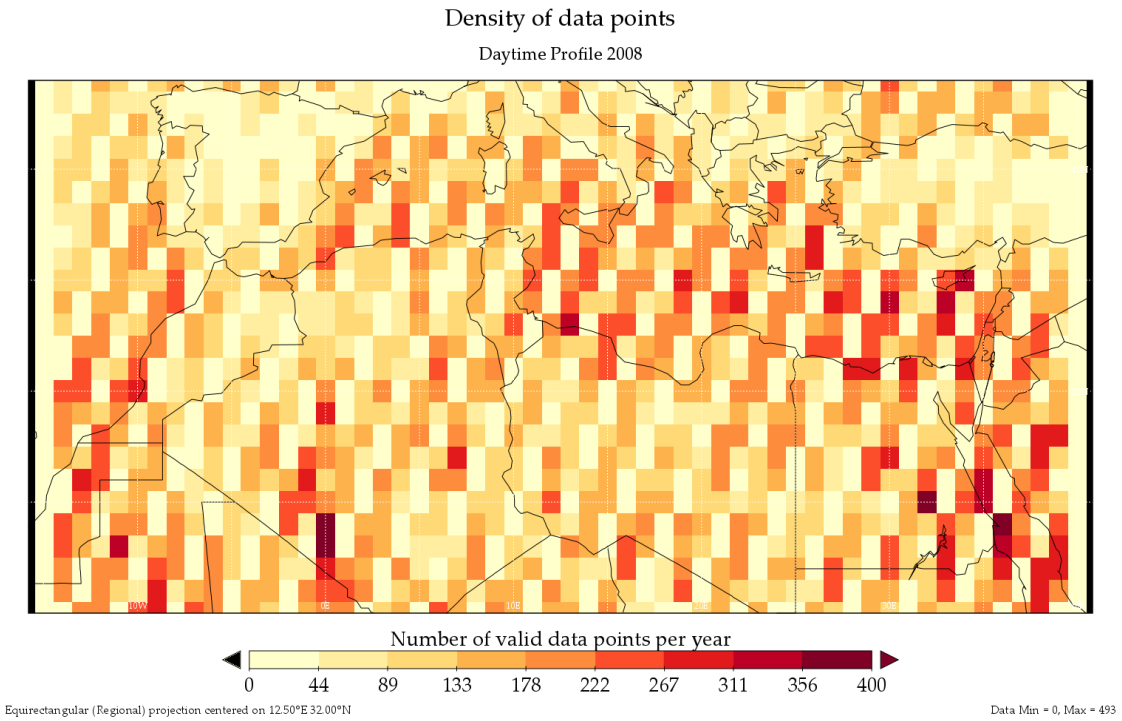

Figure 5.12

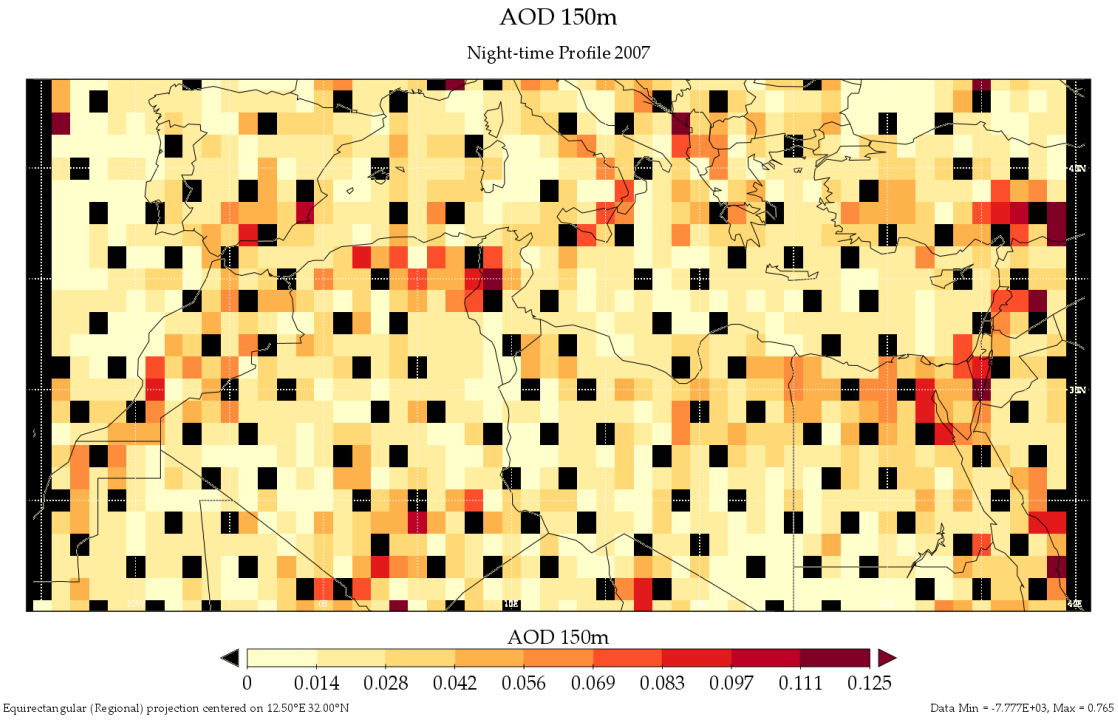

Figure 5.13

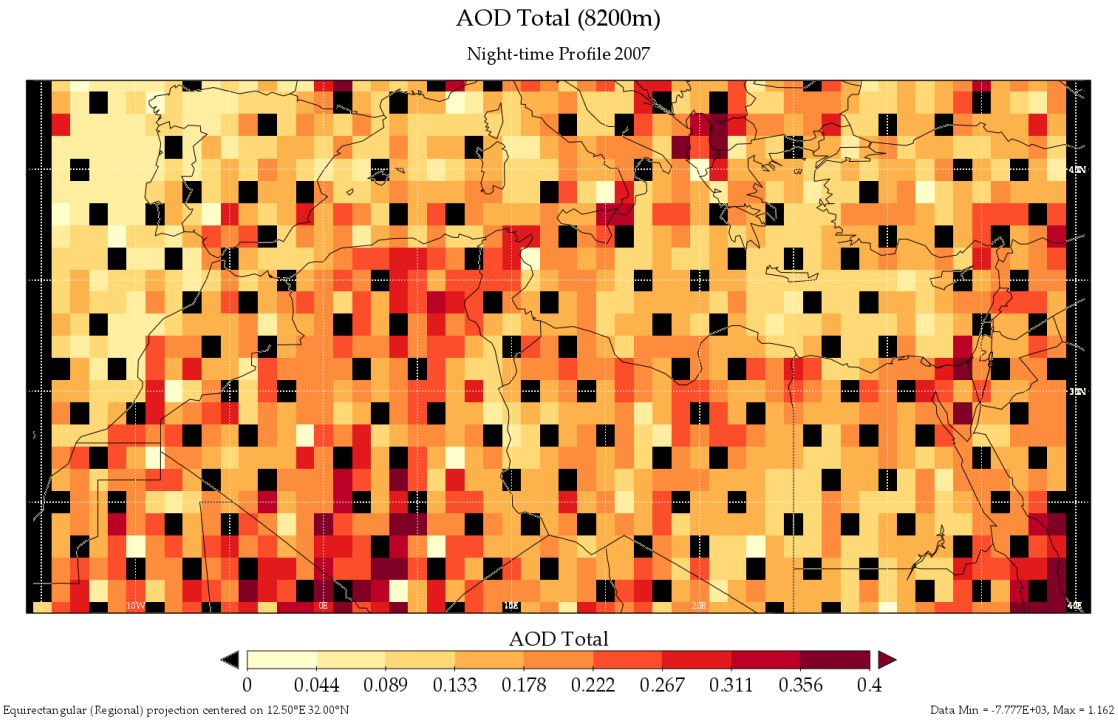

Figure 5.14

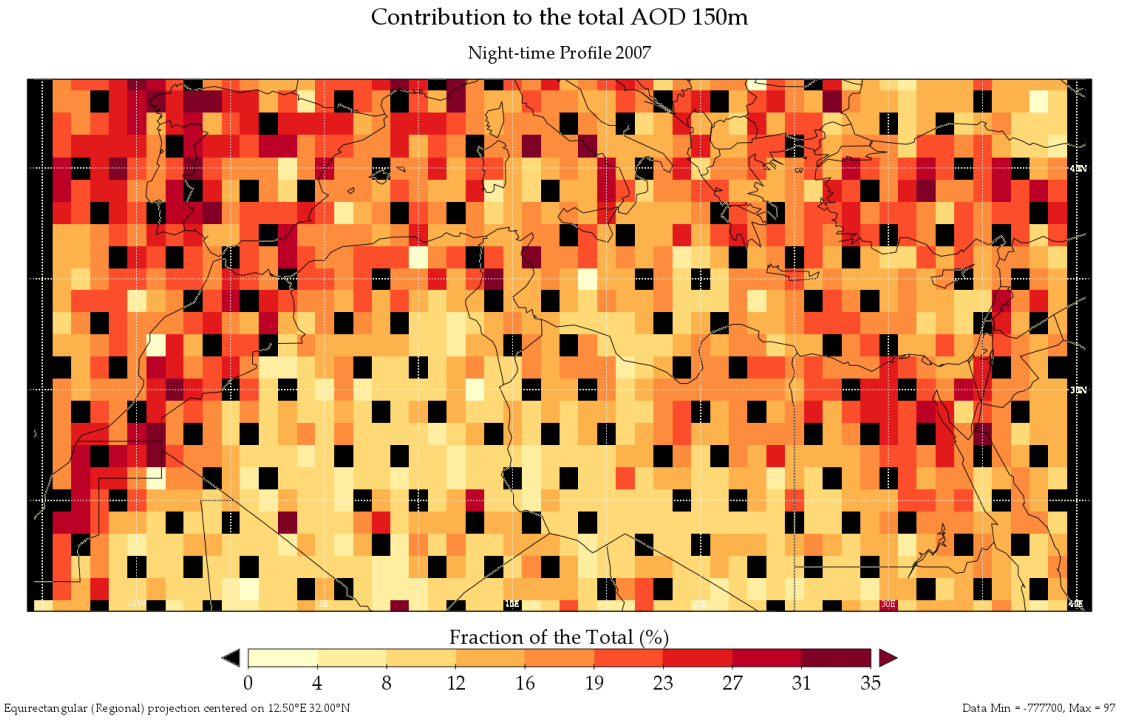

Figure 5.15

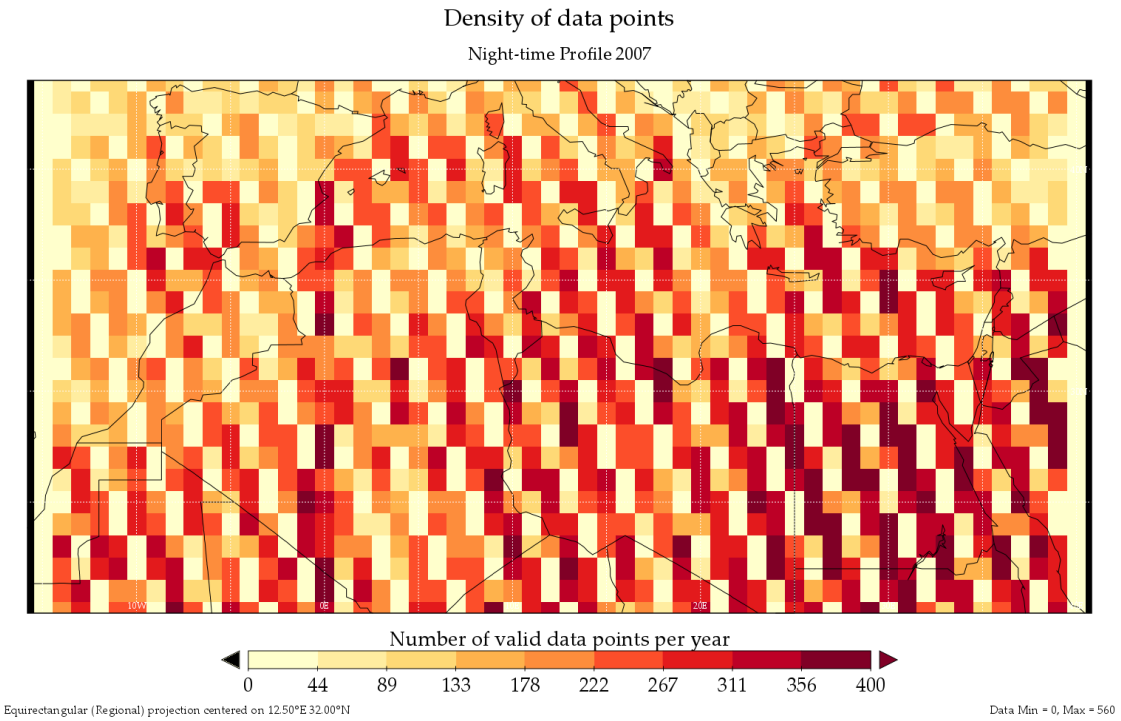

Figure 5.16

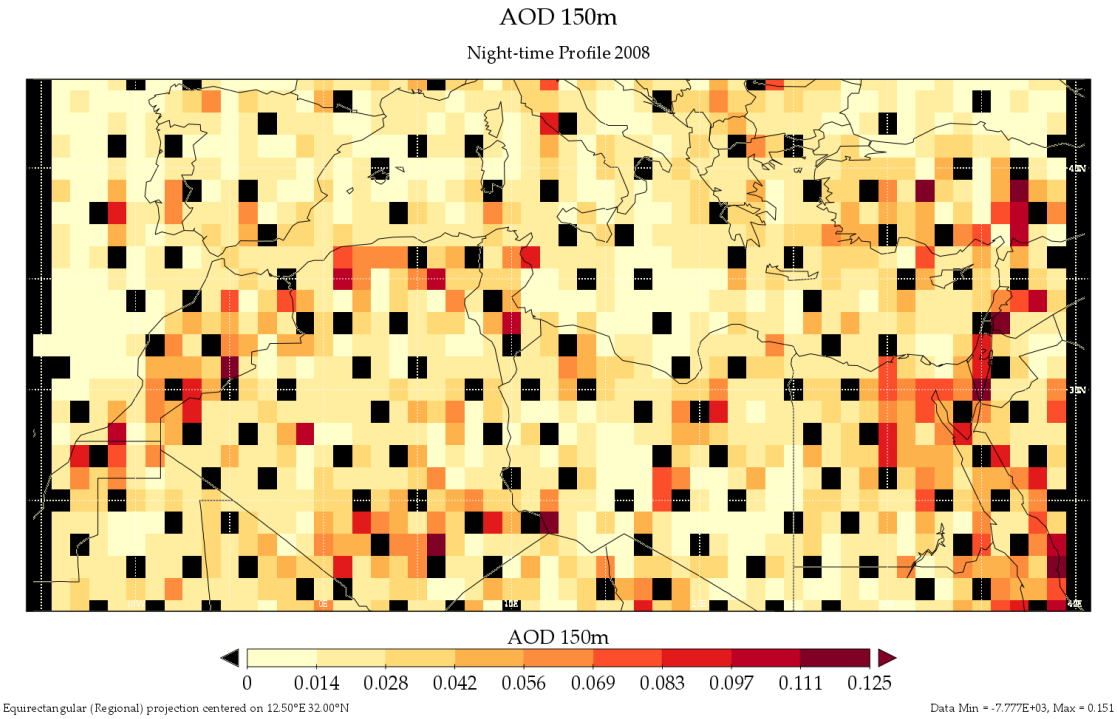

Figure 5.17

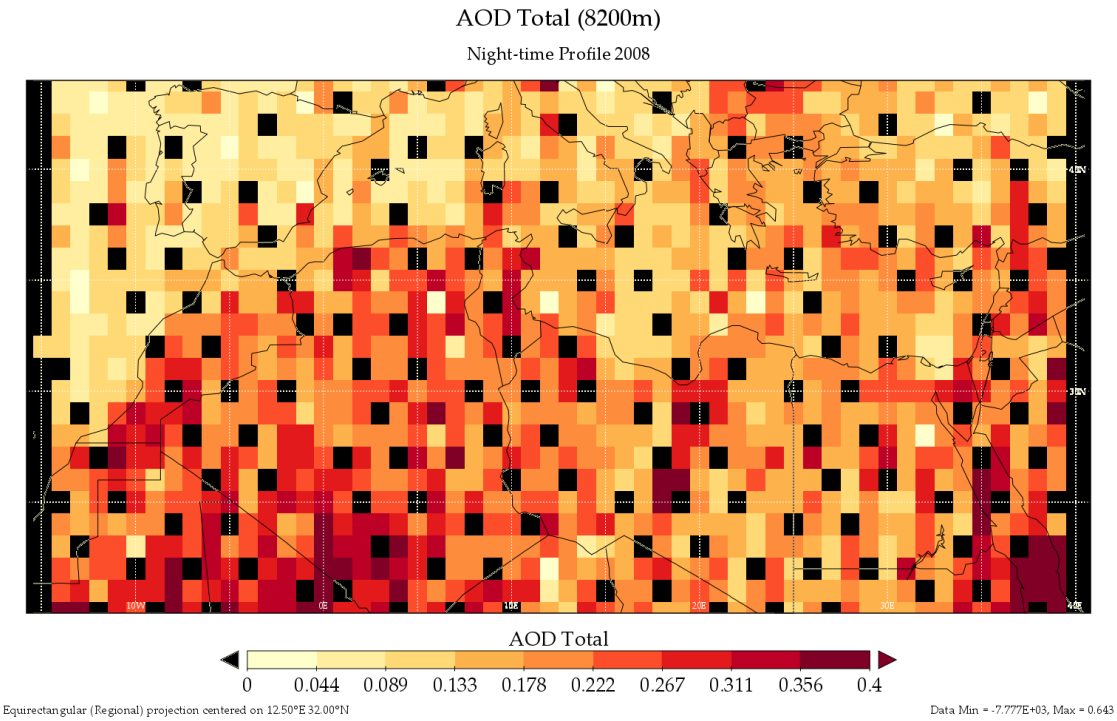

Figure 5.18

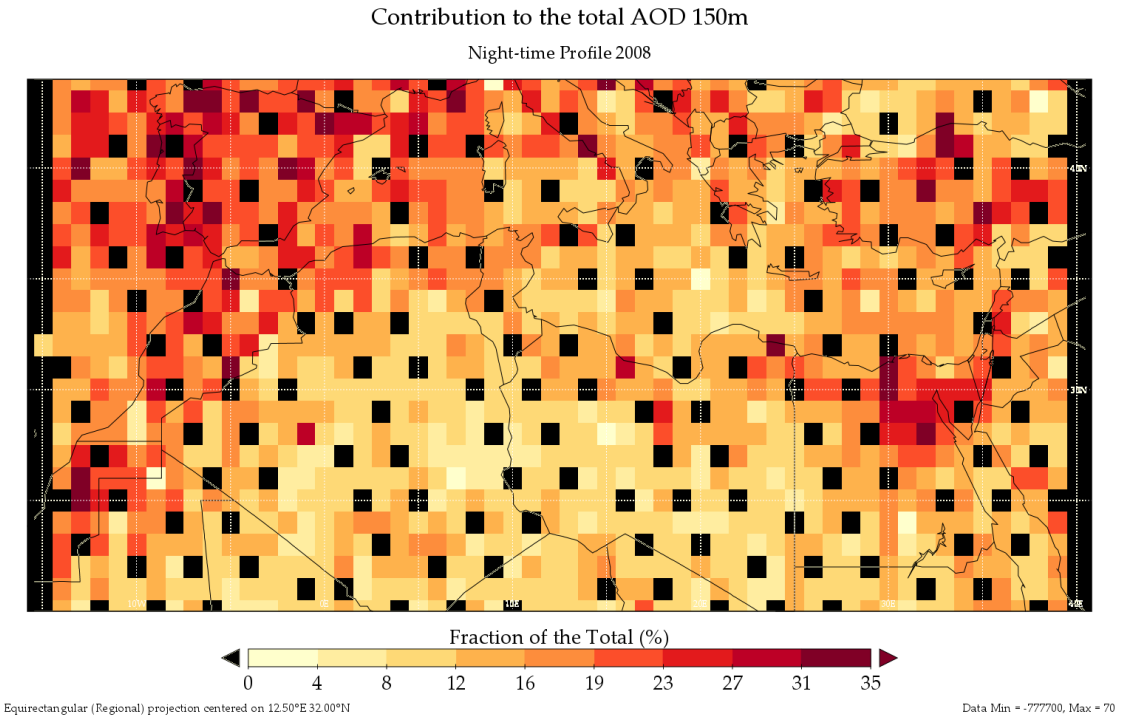

Figure 5.19

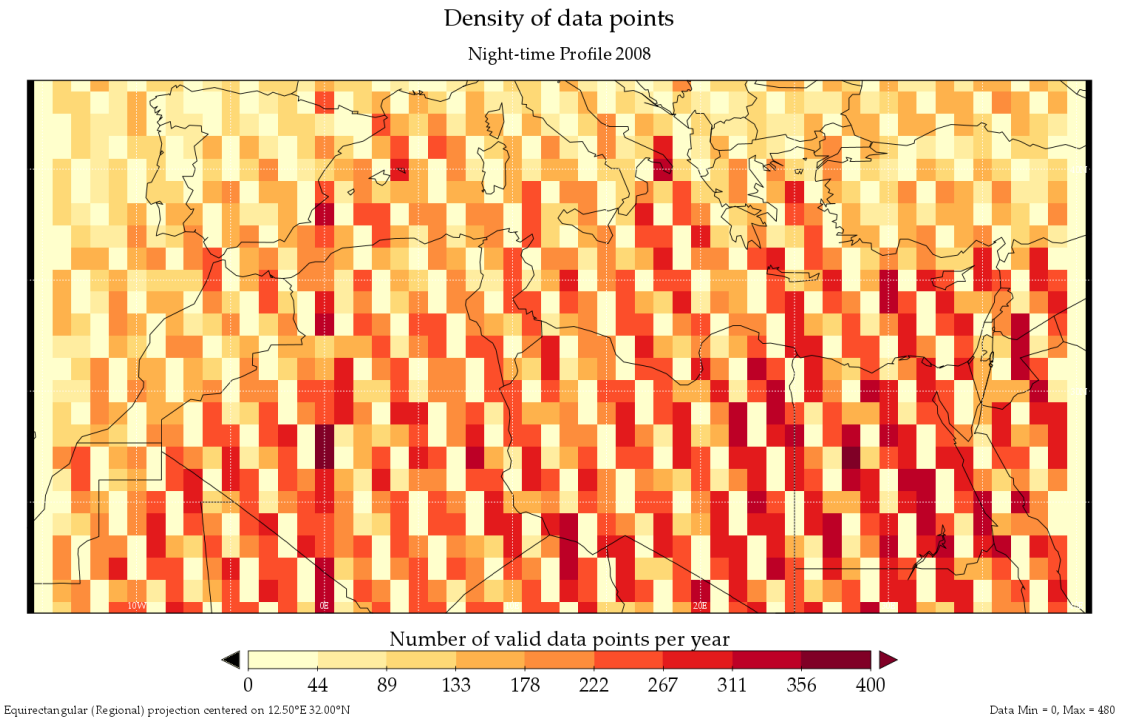

Figure 5.20

the considered total column (8 200m) the behavior is relatively the same for 2007 and 2008, with some slight differences. Regional patterns are clearer that in the 150m graphs and again, the night profiles show a general tendency of enhancing of values compared to the day. In 2007, during the day the highest contributions in the lowest layer are encountered along the Atlantic coasts of the Iberian Peninsula and Morocco, in Northwest and Northeast Spain, the French Riviera, the Alboran Sea and some regions in Turkey. During night in the same year the contribution of AOD in 150m increases considerably compared to day values in Turkey, the continental part of Spain, the coast of the Tyrrhenian Sea, North Algeria, Tunisia, the coast of Balkans at the Adriatic Sea and the most significant rise is found in Northeast Egypt and the south part of Morocco. In 2008 the highest points in the day profile remains in Portugal, the Atlantic coasts of Portugal and Spain, the French Riviera and Morocco. In the same way as the behavior observed in 2007, the contribution of AOD in the first 150m during night compared to daytime values in 2008, is intensified in Morocco, Spain, Turkey, North Algeria, the Adriatic coast of the Balkans visibly higher in the Northeast part of Egypt.

In general it might be said that the total AOD for 2008 was slightly higher than that in 2007. In the plots it is possible to observe for both years that unlike AOD in 150m and AOD ratio this set of points seems to have higher values during day than at night (see North Mali, North Mauritania, Turkey) with exception of Northeast Egypt, Israel and Syria where the tendency seems to follow a slight rise during night. However this change in values is slightly less noticeable in 2008.

The Northern Mauritania, Northern Mali, Algeria (mainly south), Turkey, Balkan Peninsula, Tunisia, central Libya, the Nubian Desert in Eastern Sahara and the Red Sea adjoining the North Sudan coasts are the areas with the higher total values of AOD along 8.2km above ground for both years. In 2007 in Spain and Portugal there is not a clear difference between day and night. Besides the already mentioned general tendency of aerosol to rise at night especially in the zones with high values, it is substantial the amount of total AOD in the surrounding east Sicily mainly in 2007.

CHAPTER 6

Discussion

Going back to the concerns disscussed in chapter 1 about investment in CSP plants, and after progressing to this point of the study, there are more elements now to evaluate the possible input of this work in the light of the industry's needs. From the point of view of investors, regarding atmospheric issues, information must be translated into a metric that represents net energy loss over certain period of time. So far this has not been completed for the suspended aerosols. This study is the first attempt to supply in a less costly way information about the aerosol distribution in the working space of a tower CSP plant. However, further analysis has to be realized in order to quantify the effect of these particles in the energy yield.

Despite being an effort to quantify the aerosols with regard to solar energy applications, it is also interesting to see this work from the perspective of its general behavior in the night, even if this is of low interest to the CSP industry.

By observing the areas where the highest values of total AOD comes from, it might be said that it belongs mostly to desert regions. Over there it can be presumed that the aerosol is of dust nature mainly. The mentioned highlighted zones correspond to North African dust sources compiled among which are: West

Africa(WA source, covering large areas of Mauritania, Mali and South Algeria), North-West Africa (NWA source, from south of Atlas Mountains to central Algeria), the Libyan Desert and the Nubian Desert(Sudan) [Engelstaedter et al., 2006]. Some of these sources were also recognized and studied by airborne campaign by [Ryder et al., 2012]. The figure 6.1 illustrates the long term (between 1980 and 1992) dust sources identified by Engelstaedter with the help of TOMS AI measurements.

Regarding the described slight rise of total AOD during night, it seems to be accompanied by a redistribution of loads in the diurnal/night-time patterns. It would be required a more detailed analysis to quantify the change and determining whether it is due to a rearrangement of particles or whether there is clear tendency to flow differentiated in the day/night cycles. The meaning or possible explanation is probably more related with wind regimens or transport patterns and it is not on the scope of this study.

However, although regions like Turkey, Spain and the Adriatic coast of the Balkans are not known as being arid, they appear in the graph as significant contributors to the highest values of AOD in the 150m above the ground. It could be attributed to other possible reasons like:

- Dust transport: by means of satellite imagery and atmospheric dust concentration measurements three major pathways for dust transport from North African sources have been identified: across the Atlantic Ocean to the United States, the Caribbean and South America, towards the central Mediterranean and Europe and towards the eastern Mediterranean and Europe [Engelstaedter et al., 2006].

  From the first path, dust can reach the Iberian peninsula, from the second and third dusty conditions can be produced in the Mediterranean indicated regions. According to [Kaskaoutis et al., 2012] the measurements of the trajectory of dust storms from the Sahara Desert towards the Mediterranean made in their study suggest the gravitational settling of the dust particles from the upper levels into the lower boundary layer as the dust moves away the source, as

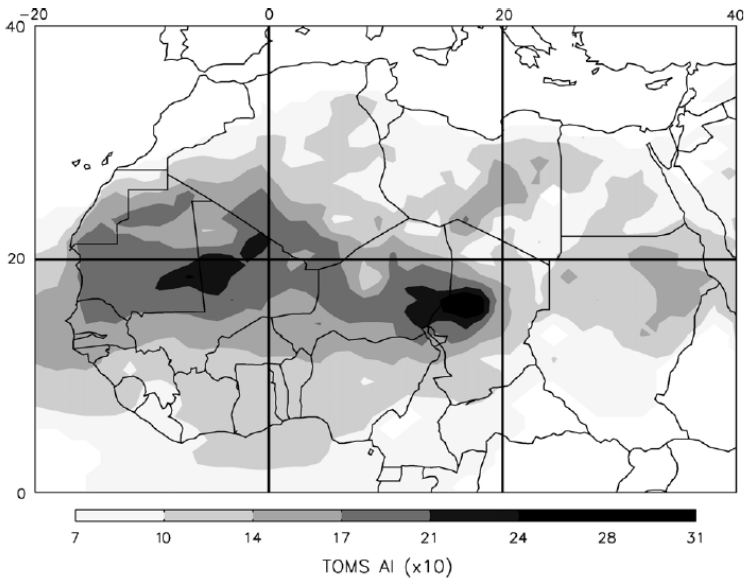

Figure 6.1: Long term (between 1980 and 1992) dust sources identified with the help of TOMS AI REF. [Engelstaedter et al., 2006].

well as the changes that their properties can exhibit after mixing with other aerosols in the atmosphere.

- Pollution and volcanic ashes (for instance in the case of the metropolitan area of Cairo, north Italy and south Italy correspondingly). Activity in Mount Etna was reported in 2007-2008 by [Aiuppa et al., 2010].

- Anthropogenically modified sources: [Engelstaedter et al., 2006] also references this concept that defines the dust resultant of disturbed soils by means of activities like agriculture, mining and water management among others.

- Aerosols due to combustion of biomass by anthropogenic activity normally present in the subsaharian region could have effect in the analized region because of transport. On the other hand wildfire episodes could have caused particulate presence in regions like Spain, Portugal, France and Greece with influence in the neighbourhood.

- Barren and arid plateaus present in those areas that could be sources of dust with different characteristics and minor loadings.

In the same manner the influence of some events could have been reflected in the values of total AOD. For example [Nicolae et al., 2008] have documented two case studies of 2007 in which they studied both the presence and evolution of smoke in Bucharest and Athens due to forest fires in Ukraine and Moldavia and the effect of desert aerosols from Africa observed from the same stations. The altitudes registered for the abovementioned events oscillate between 2 000 and 3 000m, so that their contributions would belong to the whole vertical column.

On the other hand, the general tendency of rise of the AOD in the lowest layers at night could be explained by the shallow inversion of the temperature produced when near-surface layer cools because the heat source (the sun) is not providing radiation and the stored energy escapes. Facing the absence of the heat that produces convection, the particulate matter undergoes a subsidence what is reflected in the raising of levels of AOD in the lowest layer at night. In the light of this diurnal/night cycle of temperatures it could be understood the fact that over water bodies the presence of aerosols in the 150m relative to the total (see Atlantic coast segment and Mediterranean spots) seems to have a constant base value. This might suggests that aerosols standing in the near water-surface stay without the drastic dynamic of lifting typically observed continental zones. It might be explained because the lower thermal inertia of water compared to land. Although sea spray and sea salt are also considered dominant in the remote oceans in absence of significant transport of continental aerosol, some of this marine aerosols might contribute to the share of particles over these areas.

Complementary information can be acquired from the total AOD plots. They show that compared to desert regions, water bodies and most of the rest of zones with highest concentrations of aerosol in the lowest layers (described at the beginning of this section) are not the regions with the highest absolute contribution of aerosol in the complete analyzed region. It means that for these regions the major part of aerosols are located in the lowest layers.

From an analysis of these observations three categories of areas are defined with

regard to solar tower plants:

I - HiLo Places where the largest part of aerosols are concentrated in the lowest 150m. Places like Portugal where AOD ratio is higher would face the scenario in which the solar irradiation that reaches the top of the 150m above the ground is much less extinct since it is assumed that the particles in the upper part have the minimum contribution compared with the other categories.

II - LoHi Places like the frontier of Libya that borders Algeria where the value of AOD in the first 150m is not the highest but the total AOD is in the higher scale. There although the presence of aerosols near-ground is not in itself large the incoming irradiation that reaches the top of that layer is diminished by the dense layer of matter above it.

III - HiHi Places like southern Algeria (generally categorized as dust sources) where high densities of particles can be encountered in both lowest and higher layers. In that case besides the already significantly diminished radiation reaching the near-surface troposphere CPS installations would have to face the effects of a local high density of particles on the operation of performance of the plants. For the case of dust aerosols according to Ryder it seems that the largest particles (effective diameter larger than 12μm) are present close to the source but are not transported much further afield. They are mainly encountered within 1km and a large fraction of these were within 100m of the ground [Ryder et al., 2012]. It has implications not only in the extinction of the irradiance but also in issues of maintenance of the heliostats and the general system.

The table 6.1 illustrates the mentioned categories.

	I	II	III
Higher Layer (150m - 8 200m)	○	●	●
Lower Layer (Ground - 150m)	●	○	●
Category Name	HiLo	LoHi	HiHi

Table 6.1: Categories of areas according vertical distribution of aerosols (○= weak, ●= strong).

In general, it could be observed that water bodies belong to the category HiLo. Although there is a permanent presence of aerosols in the low atmosphere, the total AOD is low compared to desert zones, so giving to the shores certain advantages from the point of view of lower total AOD. Then the closeness to the sea would reduce the amount of particulate matter improving presumably the conditions for the operation of CSP plants. Of course, certain local effects (like condensation) and the nature of aerosols might compensate or even counteract the low- particle conditions at the shore regarding the performance of the plant. This aspect is beyond the scope of the present study.

As can be seen in the maps night profiles have noticeably higher values in the AOD 150m and ratio maps. Thus, in general, differences between day and night patterns allows to state that solar applications do not face the worst case in the near-surface layer (150m).

The series of graphs that describe the density of valid points shows that in general 2007 had more valid points compared to 2008. The difference is more significant in longitudes from 10°E to 40°E. This could be explained by two main reasons. First of all the available CALIPSO source files for the chosen region in 2007 were 10 157 against 9 727 in 2008. Taking into account that for every file there is an average of 3 700 geographical points that could belong to the region of interest, it would mean that there would be around 1 600 000 profiles more compared to 2008. Besides the fact of having a lower average cloud fraction in the desert regions of North Africa

and the Arabian Peninsula as showed by NASA[a] provides a higher possibility of retrieving valid profiles in these regions according with the rules established for the treatment of satellite data in this study (see chapter 4). The clearly visible difference of density of points between day and night is mainly attributed to the fact of that noise levels in the daytime measurements are much larger than those at night. This is due to the solar background signal that complicates the retrieval of reliable data.

Concerning the uncertainties, the expected error for each cell (not estimated here) is not be as high as the individual values of uncertainty presented in the section 5.2. This is because it is the error of a mean. However given the order of magnitude of these indivual readouts in such a lower values, in order to minimize the noise artifacts a color palette of only 9 levels was selected. As a result less amount of values can be distinguished.

According to NASA the levels of uncertainties in the retrieved information are associated to several factors, among which are:

Intensity of signal Strongly scattering features are easier to detect that weakly scattering features.

Signal/Noise ratio Due to solar background daytime measurements are much larger than those at night.

Increasing Optical Depth The larger the optical depth above the feature the more difficult is the detection because the laser light must pass through a thicker layer.

Multiple Scattering It is the phenomenon wherein photons scattered from the feature are re-scattered from neighbouring particles prior to reach the instrument detector. An illustrative sketch can be observed in 6.2.

Use of PDF in the CAD algorithm As referred in section 4.1the discrimination between aerosols and clouds is carried out with help of probabilistic func-

[a] `http://earthobservatory.nasa.gov/GlobalMaps/view.php?d1=MODAL2_M_CLD_FR`

tions that inherently have an associated uncertainty[b].

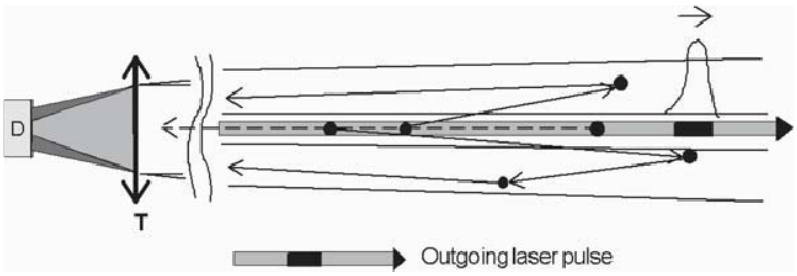

Figure 6.2: Multiple Scattering in the LIDAR geometry. The grayline represents the outgoing laser pulse, the arrows are the scattering events [Weitkamp, 2005].

In conclusion it is possible to highlight the achievements of:

1. Exploring previous studies of vertical structure of aerosols carried out by means of different techniques like in-situ measurements, remote sensing and numerical models and concluding that in spite of the different efforts there is still a need of characterization of aerosols in the lowest troposphere.

2. Depicting the effect of the presence of aerosols in a relevant altitude for CSP tower plants (150m) with the help of the active instrument of CALIOP (LIDAR) to profile vertically the atmosphere.

In order to make the present and future findings about aerosol effects applicable to solar plants three complementary approaches might be tackled:

From local evaluation Further research must be focused on the more detailed local evaluation of vertical and horizontal distribution of aerosols in the relevant volume where solar plants operate. Optical interferences and final effects of each particle possibly presented with light must be characterized. If possible establishing a standardized method that allows a quick and precise characterization of atmospheric local conditions.

From remote sensing Since remote sensing is an alternative to the costly, time-demanding methods to describe local conditions it might be considered as

[b] http://eosweb.larc.nasa.gov/PRODOCS/calipso/Quality_Summaries/CALIOP_L2LayerProducts_3.01.html#he

a useful tool that can provide global coverage of information in an effective time and less expensive way if sufficient accurate observations and statistically significant amount of data can be acquired.

From numerical models Given the flexibility to simulate nearly every parameter, models have been evolving in the capacity of reproducing metereological conditions and processes but they need to be validated. For such validation due to its spatial uniformity, satellite data seems to represent an appropriate alternative.

In summary, the present study is a starting point to characterize more precisely the influence of aerosols in the performance of solar plants and to evaluate the usefulness of available vertical aerosol data for this purpose. In the choice of a strategic location for solar plants this study can serve as initial guide at considering atmospheric conditions as one of the relevant factors of operation and performance for these systems. The results presented can be used as well as complement for information retrieved by passive remote sensing techniques, like in the case of solar energy prospection, where the aerosols are taken as input in the model of determination of irradiation hitting the surface.

Bibliography

[Abengoa, 2009] Abengoa (2009). PS20, the second solar power tower worldwide. `http://www.abengoasolar.com`.

[Ackerman and Cox, 1982] Ackerman, S. and Cox, S. (1982). The saudi arabian heat low: Aerosol distributions and thermodynamic structure. *Journal of Geophysical Research: Oceans*, 87(C11):8991–9002.

[Aiuppa et al., 2010] Aiuppa, A., Cannata, A., Cannav, F., Di Grazia, G., Ferrari, F., Giudice, G., Gurrieri, S., Liuzzo, M., Mattia, M., Montalto, P., Patan, D., and Puglisi, G. (2010). Patterns in the recent 2007 - 2008 activity of mount etna volcano investigated by integrated geophysical and geochemical observations. *Geochemistry, Geophysics, Geosystems*, 11(9):n/a–n/a.

[Barnum et al., 2004] Barnum, B., Winstead, N., Wesely, J., Hakola, A., Colarco, P., Toon, O., Ginoux, P., Brooks, G., Hasselbarth, L., and Toth, B. (2004). Forecasting dust storms using the carma-dust model and MM5 weather data. *Environmental Modelling and Software*, 19(2):129–140.

[Bösenberg and Matthias, 2003] Bösenberg, J. and Matthias, V. (2003). Report no.348 EARLINET: An European Aerosol Research Lidar Network to Establish an Aerosol Climatology. Technical report, Max-Planck-Institute für Meteorology.

[Chung, 2012] Chung, C. E. (2012). *Atmospheric Aerosols Regional Characteristics Chemistry and Physics*, chapter Aerosol Direct Radiative Forcing: A Review. InTeOp.

[Engelstaedter et al., 2006] Engelstaedter, S., Tegen, I., and Washington, R. (2006). North african dust emissions and transport. *Earth-Science Reviews*, 79(1-2):73 – 100.

[Ginoux et al., 2001] Ginoux, P., Chin, M., Tegen, I., Prospero, J. M., Holben, B., Dubovik, O., and Lin, S.-J. (2001). Sources and distributions of dust aerosols simulated with the gocart model. *Journal of Geophysical Research: Atmospheres*, 106(D17):20255–20273.

[Gobbi et al., 2000] Gobbi, G. P., Barnaba, F., Giorgi, R., and Santacasa, A. (2000). Altitude-resolved properties of a saharan dust event over the mediterranean. *Atmospheric Environment*, 34(29-30):5119 – 5127. Sixth Scientific Conference of the International Global Atmospheric.

[Heinemann, 2010] Heinemann, D. (2010). *Energy Meteorology*. Springer.

[Hodzic et al., 2004] Hodzic, A., Chepfer, H., Vautard, R., Chazette, P., Beekmann, M., Bessagnet, B., Chatenet, B., Cuesta, J., Drobinski, P., Goloub, P., Haeffelin, M., and Morille, Y. (2004). Comparison of aerosol chemistry transport model simulations with LIDAR and sun photometer observations at a site near paris. *Journal of Geophysical Research: Atmospheres*, 109(D23):n/a–n/a.

[Intra and Tippayawong, 2008] Intra, P. and Tippayawong, N. (2008). An overview of differential mobility analyzers for size classification of nanometer-sized aerosol particles. *Songklanakarin Journal of Science and Technology*, 30(2):243 – 256.

[IRENA, 2012] IRENA (2012). Renewable power generation costs 2012: an overview. Technical report, International Renewable Energy Agency IRENA.

[Kaskaoutis et al., 2012] Kaskaoutis, D. G., Prasad, A. K., Kosmopoulos, P. G., Sinha, P. R., Kharol, S. K., Gupta, P., El-Askary, H. M., and Kafatos, M. (2012).

Synergistic use of remote sensing and modeling for tracing dust storms in the mediterranean. *Advances in Meteorology*.

[Knippertz et al., 2011] Knippertz, P., Tesche, M., Heinold, B., Kandler, K., Toledano, C., and Esselborn, M. (2011). Dust mobilization and aerosol transport from west africa to cape verdea meteorological overview of samum-2. *Tellus B*, 63(4).

[Liu et al., 2010] Liu, Z., Kuehn, R., Vaughan, M., Winker, D., Omar, A., Powell, K., Trepte, C., Hu, Y., and Hostetler, C. (2010). The CALIPSO cloud and aerosol discrimination: Version 3 algorithm and test results. Technical report, National Institute of Aerospace, Hampton, VA, USA.

[NASA, 2011] NASA (2011). CALIPSO Data Products Catalog Ver 3.4. `http://www-calipso.larc.nasa.gov/products/CALIPSO_DPC_Rev3x4.pdf`.

[Navas-Guzmán et al., 2011] Navas-Guzmán, F., Guerrero-Rascado, J. L., and Alados-Arboledas, L. (2011). Retrieval of the LIDAR overlap function using raman signals. *Opt. Pura Apl.*, 44:71–75.

[Nicolae et al., 2008] Nicolae, D., Talianu, C., Mamouri, R. E., Carstea, E., Papayannis, A., and Tsaknakis, G. (2008). Air mass modification processes over the balkans area detected by aerosol lidar techniques. *Optoelectron. Adv. Mat.*, 2/6:405 – 412.

[Nishizawa et al., 2010] Nishizawa, T., Sugimoto, N., Matsui, I., Shimizu, A., Liu, X., Zhang, Y., Li, R., and Liu, J. (2010). Vertical distribution of water-soluble, sea salt, and dust aerosols in the planetary boundary layer estimated from two-wavelength backscatter and one-wavelength polarization LIDAR measurements in guangzhou and beijing, china. *Atmospheric Research*, 96(4):602 – 611.

[Pérez et al., 2006a] Pérez, C., Nickovic, S., Baldasano, J. M., Sicard, M., Rocadenbosch, F., and Cachorro, V. E. (2006a). A long saharan dust event over the

western mediterranean: Lidar, sun photometer observations, and regional dust modeling. *Journal of Geophysical Research: Atmospheres*, 111(D15):n/a–n/a.

[Pérez et al., 2006b] Pérez, C., Nickovic, S., Pejanovic, G., Baldasano, J. M., and Özsoy, E. (2006b). Interactive dust-radiation modeling: A step to improve weather forecasts. *Journal of Geophysical Research: Atmospheres*, 111(D16):n/a–n/a.

[Petzold et al., 2011] Petzold, A., Veira, A., Mund, S., Esselborn, M., Kiemle, C., Weinzierl, B., Hamburger, T., Ehret, G., Lieke, K., and Kandler, K. (2011). Mixing of mineral dust with urban pollution aerosol over Dakar (Senegal): impact on dust physico-chemical and radiative properties. *Tellus B*, 63(4).

[Prospero et al., 2002] Prospero, J. M., Ginoux, P., Torres, O., Nicholson, S. E., and Gill, T. E. (2002). Environmental characterization of global sources of atmospheric soil dust identified with the nimbus 7 total ozone mapping spectrometer (toms) absorbing aerosol product. *Reviews of Geophysics*, 40(1):2–1–2–31.

[Ramanathan, 2006] Ramanathan, V. (2006). Western pacific autonomous uav campaign - aerosol-dust-cloud interactions and climate effects. Technical report, Scripps Institution of Oceanography, University of California, San Diego.

[Ramanathan et al., 2008] Ramanathan, V., Agrawal, M., Akimoto, H., Auffhammer, M., Autrup, H., Barregard, L., Bonasoni, P., Brauer, M., Brunekreef, B., Carmichael, G., Chang, W.-C., Chopra, U. K., Chung, C., Devotta, S., Duffus, J., Emberson, L., Feng, Y., Fuzzi, S., Gordon, T., Gosain, A., Hasnain, S., Htun, N., Iyngararasan, M., Jayaraman, A., Jiang, D., Jin, Y., Kalra, N., Kim, J., Lawrence, M. G., Mourato, S., Naeher, L., Nakajima, T., Navasumrit, P., Oki, T., Ostro, B., Panwar, T. S., Rahman, M., Ramana, M., Rodhe, H., Ruchirawat, M., Rupakheti, M., Settachan, D., Singh, A. K., Helen, G. S., Tan, P. V., Tan, S., Viet, P., Vincent, J., Wang, J., Wang, X., Weidemann, S., Yang, D., Yoon, S., Zelikoff, J., Zhang, Y., and Zhu, A. (2008). Atmospheric brown clouds: Regional assessment report with focus on asia. Technical report, United Nations Environment Programme, Nairobi, Kenya.

[Ryder et al., 2012] Ryder, C. L., Highwood, E. J., Rosenberg, P. D., Trembath, J., Brooke, J. K., Bart, M., Dean, A., Crosier, J., Dorsey, J., Brindley, H., Banks, J., Marsham, J. H., McQuaid, J. B., Sodemann, H., and Washington, R. (2012). Optical properties of saharan dust aerosol and contribution from the coarse mode as measured during the fennec 2011 aircraft campaign. *Atmospheric Chemistry and Physics Discussions*, 12(10):26783–26842.

[Schmechtig et al., 2011] Schmechtig, C., Marticorena, B., Chatenet, B., Bergametti, G., Rajot, J., and Coman, A. (2011). Simulation of the mineral dust content over western africa from the event to the annual scale with the chimere-dust model. *Atmospheric Chemistry and Physics*, 11(14):7185–7207.

[Slingo et al., 2008] Slingo, A., Bharmal, N. A., Robinson, G. J., Settle, J. J., Allan, R. P., White, H. E., Lamb, P. J., Lélé, M. I., Turner, D. D., McFarlane, S., Kassianov, E., Barnard, J., Flynn, C., and Miller, M. (2008). Overview of observations from the radagast experiment in Niamey, Niger: Meteorology and thermodynamic variables. *Journal of Geophysical Research: Atmospheres*, 113(D13):n/a–n/a.

[Su and Toon, 2009] Su, L. and Toon, O. B. (2009). Numerical simulations of asian dust storms using a coupled climate-aerosol microphysical model. *Journal of Geophysical Research: Atmospheres*, 114(D14):n/a–n/a.

[Toon et al., 1988] Toon, O. B., Turco, R. P., Westphal, D., Malone, R., and Liu, M. (1988). A multidimensional model for aerosols: Description of computational analogs. *Journal of the Atmospheric Sciences*, 45(15):2123–2144.

[Torresol_Energy, 2011] Torresol_Energy (2011). Brochure of Gemasolar power plant. `http://www.torresolenergy.com`.

[Trieb et al., 2009] Trieb, F., Schillings, C., O'Sullivan, M., Pregger, T., and Hoyer-Klick, C. (2009). Global potential of concentrating solar power. In *Proceedings of SOLARPACES conference - Berlin 2009*.

[Turco et al., 1979] Turco, R. P., Hamill, P., Toon, O. B., Whitten, R. C., and Kiang, C. S. (1979). A one-dimensional model describing aerosol formation and evolution in the stratosphere: I. physical processes and mathematical analogs. *Journal of the Atmospheric Sciences*, 36(4):699–717.

[Vuolo et al., 2009] Vuolo, M. R., Chepfer, H., Menut, L., and Cesana, G. (2009). Comparison of mineral dust layers vertical structures modeled with chimere-dust and observed with the caliop LIDAR. *Journal of Geophysical Research: Atmospheres*, 114(D9):n/a–n/a.

[Weitkamp, 2005] Weitkamp, C., editor (2005). *LIDAR. Range-Resolved Optical Remote Sensing of the Atmosphere*. Springer.

[Winker, 2006] Winker, D. (2006). First experiences with CALIOP. `http://esamultimedia.esa.int/docs/5-1_Winker.pdf`.

[Witschas, 2012] Witschas, B. (2012). *Atmospheric Physics*, chapter Light Scattering on Molecules in the Atmosphere. Springer.